Title

MEASUREMENT OF LIFETIMES BY THE PHASE-SHIFT METHOD. I. RADIATIVE LIFETIMES OF SOME EXCITED ATOMIC STATES. II. LIFETIMES OF SOME v' REGIONS OF THE B3no+u STATE OF I2

Author

Cunningham, Paul T.

Publication Date

1968-11-01

UCRL-18419

cy.2

MEASUREMENT OF LIFETIMES BY THE PHASE-SHIFT METHOD

I. RADIATIVE LIFETIMES OF SOME EXCITED ATOMIC STATES

II. LIFETIMES OF SOME v' REGIONS OF THE $B^3\Pi_{0^+u}$ STATE OF I_2

Paul T. Cunningham
(Ph.D. Thesis)

November 1968

LRL

LAWRENCE RADIATION LABORATORY
UNIVERSITY of CALIFORNIA BERKELEY

UCRL-18419

cy.1

DISCLAIMER

UCRL-18419

UNIVERSITY OF CALIFORNIA

Lawrence Radiation Laboratory
Berkeley, California

AEC Contract No. W-7405-eng-48

MEASUREMENT OF LIFETIMES BY THE PHASE-SHIFT METHOD

I. RADIATIVE LIFETIMES OF SOME EXCITED ATOMIC STATES
II. LIFETIMES OF SOME v' REGIONS OF THE $B^3\Pi_{0^+u}$ STATE OF I_2

Paul T. Cunningham

(Ph.D. Thesis)

November 1968

TABLE OF CONTENTS

MEASUREMENT OF LIFETIMES BY THE PHASE-SHIFT METHOD

I. RADIATIVE LIFETIMES OF SOME EXCITED ATOMIC STATES
II. LIFETIMES OF SOME v' REGIONS OF THE $B^3\Pi_{0^+u}$ STATE OF I_2

Paul T. Cunningham

Inorganic Materials Research Division, Lawrence Radiation Laboratory
Department of Chemistry,
University of California, Berkeley, California

ABSTRACT

The phase-shift technique has been used to measure radiative lifetimes for excited atomic states of eleven elements. Data were obtained over a large enough range of fluorescence radiance to permit evaluation of the effects of radiation entrapment and scattered exciting radiation. The following results were obtained: Al 4s $^2S_{1/2}$ 7.05 nsec, Al 3d ^2D 13.7 nsec, Ga 5s $^2S_{1/2}$ 7.6 nsec, Ga 4d ^2D 7.7 nsec, In 6s $^2S_{1/2}$ 7.5 nsec, In 5d $^2D_{3/2}$ 7.9 nsec, In 5d $^2D_{5/2}$ 7.9 nsec, Tl 7s $^2S_{1/2}$ 7.65 nsec, Tl 6d $^2D_{3/2}$ 6.9 nsec, Cu 4p $^2P^o$ 7.2 nsec, Ag 5p $^2P^o_{1/2}$ 7.5 nsec, Ag 5p $^2P^o_{3/2}$ 6.7 nsec, Na 3p $^2P^o$ 16.2 nsec, Cs 7p $^2P^o_{3/2}$ 114.0 nsec, Hg 6p $^3P^o_1$ 115.0 nsec, Pb 7s $^3P^o_1$ 6.05 nsec, and Bi 7s $^4P_{1/2}$ 5.9 nsec. Estimated uncertainties range from 2% to 6%. The measured lifetimes have been converted to absorption f-values for the transitions depopulating the states studied by use of relative f-values from the literature.

Lifetime measurements have been made on the B state of I_2 excited to vibrational levels around v' ~ 15, 25 and 50. The lifetimes measured for v' ~ 25 vary with the frequency of modulation of the exciting light. The results are compared with previous measurements reported in the literature and all data interpreted in terms of a weak spontaneous predissociation of the B state.

LIST OF FIGURES

LIST OF TABLES

I. RADIATIVE LIFETIMES OF SOME EXCITED ATOMIC STATES

A. Introduction

The features of atomic and molecular spectra which are of most obvious interest are the wavelengths of the lines or features and their radiances. While wavelengths are in general known with great accuracy, radiances are known to one or at best two significant figures and are frequently characterized in qualitative terms such as strong, weak, easily observable, etc. The radiance of a spectral feature is most often quantitatively expressed in terms of the absorption f-value[1] which indicates the degree to which the transition resembles the corresponding transition for a classical elastically bound electron.

Increasing interest in accurate information on absolute radiance has been evident in recent years due to developments in the fields of plasma physics, stimulated emission, astrophysical chemical abundance, quantum chemistry, and the problems of energy transfer from space vehicles during atmospheric reentry. This new interest has led to a variety of new or improved experimental techniques which have increased the number of accurately known f-values. This improvement can perhaps be best demonstrated by examination of the advances made since the important work on atomic transition probabilities by Corliss and Bozmann[2] which was published in 1962. Using an arc with copper alloy electrodes, they determined relative f-values for over 25,000 lines of 70 elements. They then selected experimental absolute f-values for transitions in 18 elements to use as a basis for the normalization of their relative values. Since 1962 most of these selected values have been redetermined by methods which should be accurate to 10%. The only f-values they selected which are still

within 10% agreement with the best available numbers are those for the resonance transitions of the alkali metals.

It has been pointed out that the experimental methods for determining f-values can be divided into two groups,[3] those which are dependent on the concentration of the species being investigated and those which are not. The concentration dependent methods, which include magneto-rotation,[1] total absorption,[1] radiance from arcs[2] and anomalous dispersion (the hook method),[3] are based on the behavior of a particular transition between two states and give directly the product Nf, where N is the particle density, so that N must be previously known or independently determined to obtain the f-value. The concentration independent methods which include the phase shift technique, double resonance,[4] level crossing,[4] and direct observation of decay,[5,6] are based on properties of the excited state and therefore include information on all of the transitions which depopulate that state. This means that the branching ratio, the relative effectiveness of the various transitions in depopulating the state, must be known in order to obtain f-values for the transitions.

In practice, it is possible to determine the relative f-values for a large number of atomic transitions using concentration dependent techniques, particularly anomalous dispersion (the hook method), but absolute f-values obtained by these methods reflect uncertainties in vapor pressures, which are often large. On the other hand, the concentration independent techniques, particularly the method of level crossing and the phase shift method, lend themselves to accurate determination of a few selected f-values. It would seem then, that the greatest contribution to the body of accurately known radiances can be made by using the data from density independent

methods to place the relative f-values of the density dependent methods on an absolute scale. The work reported here was undertaken with this goal in mind and to demonstrate the reliability of the phase shift method.

In the phase shift method the lifetime, τ_k, of an excited state is experimentally determined. Under conditions where the atoms being investigated can be considered as isolated, as in a dilute vapor, the lifetime obtained is the radiative lifetime, τ_k°. The radiative lifetime of any state is given by

$$\tau_k^\circ = 1/\Sigma\ A_{k\ell} \qquad \text{(I-1)}$$

where $A_{k\ell}$ is the Einstein transition probability for spontaneous emission and the sum is taken over all possible transitions depopulating the state. The absorption f-value for a given transition is related to $A_{k\ell}$ for that transition by

$$f_{\ell k} = \frac{m\ c}{8\pi^2\ e^2} \cdot \frac{g_k}{g_\ell}\ \lambda_{k\ell}^2\ A_{k\ell} \qquad \text{(I-2)}$$

$$f_{\ell k} = 1.499\times10^{-14}\ \lambda_{k\ell}^2\ A_{k\ell}\ g_k/g_\ell$$

where m and e are the mass and charge of an electron respectively, c is the speed of light, λ is the wavelength of the transition in nm, and g is the statistical weight of a state. The k and ℓ subscripts indicate the upper and lower states, respectively.

In the experiments reported here the excited state is populated by radiance modulated radiant energy. The fluorescence is also modulated but delayed in phase by an amount $\Delta\phi$ which is related to the lifetime of the excited state by

$$\Delta\phi = \tan^{-1}\omega\tau \qquad \text{(I-3)}$$

where ω is the radial modulation frequency of the exciting radiant energy. A detailed discussion of this relation has been given previously[7] most recently by Chutjian.[8]

A somewhat different derivation of Eq. (I-3) is that of Lawrence.[9] He visualizes the system as being analogous to a differentiating electronic network and uses the appropriate transfer functions to obtain Eq. (I-3). This approach simplifies the analysis of phase-shift results in cases where cascading or other energy transfer processes complicate the decay process. Recently Schwartz[10] has presented a detailed discussion of these cases. The most useful discussion of the relation between uncertainties in measurement of $\Delta\phi$ and resulting uncertainties in τ is that of Bronch-Bruevich.[11]

B. Apparatus and Procedures

1. General.

The equipment used for the work reported here has evolved over a period of nearly twenty years[7,8,12-16]. Many of the components and principles of operation have been adequately described but much has been altered and improved in the present work. The intent here is to review the entire experimental setup by making reference to previous work where it is still applicable while correcting and updating the previous work where it is in error or no longer applicable. The discussion which follows will be clearer if a brief outline of the experimental technique is provided.

A block diagram of the apparatus is shown in Fig. I-1. Radiant energy from the source is modulated as it passes along the optical path. Before being focused onto the sample a portion of this radiant energy is reflected onto the reference photomultiplier thus providing a signal for the reference channel. The sample photomultiplier detects fluorescent radiant energy from the sample or scattered exciting radiant energy.

The reference channel provides a stable frequency and phase reference for the system. To make a phase shift measurement, the phase of the fluorescent radiant energy from the sample is compared to the reference phase and reference phase shifted until the phase null detector indicates a null. Fluorescence radiant energy is then replaced by scattered exciting radiant energy and the calibrated sample-phase-shifter is used to restore the phase null. The phase shift introduced by the calibrated shifter must then be equal to the shift caused by the finite lifetime of the sample. The pertinent electronic drawings are listed in the Appendix.

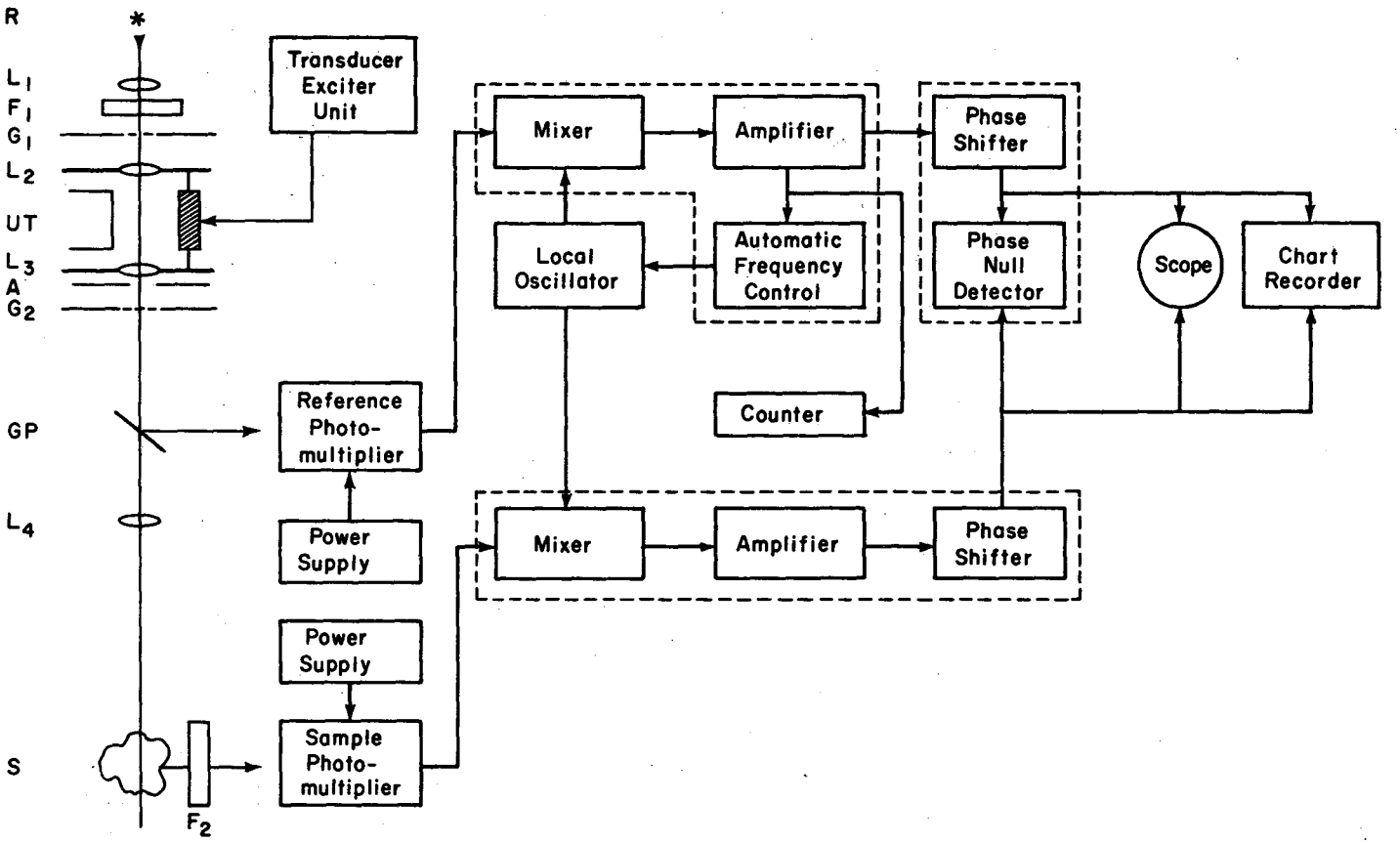

XBL 689-5942

Figure I-1

2. Optical Modulation.

The present high frequency system is operable at 5.206 MHz and at 1.000 MHz. The optical portion has been discussed by Link[16] and is essentially unchanged. The ultrasonic grating, which is the heart of the modulating system, has been redesigned so as to be more easily aligned along the optical axis and to permit rapid conversion from one frequency to another. A diagram showing this design appears as Fig. I-2. The transducer crystal is mounted in a Lucite disk (labeled E in Fig. I-2) which makes an O-ring seal with the body of the tank and forms its bottom. A water tight seal between the crystal and the Lucite is maintained by using a non-hardening sealant (Silastic RTV 891 manufactured by Dow Corning Corporation, Midland, Michigan). Conducting epoxy cement replaces the spring contacts used previously[14] as a means of making electrical contact with the water side of the crystal. The copper reflecting plate (labeled B in Fig. I-2), the purpose of which is to reinforce the standing acoustic wave in the water tank, can be easily adjusted so that the distance between it and the surface of the crystal is an exact multiple of the ultrasonic wavelength. It can also be adjusted so that its surface is parallel to that of the crystal. Details of the adjustment mechanism are not shown in Fig. I-2. Careful adjustment of the reflecting plate is necessary to achieve good diffraction patterns from the tank.

The diffraction effect of the ultrasonic tank, which was first reported by Debye and Sears[17] follows approximately the simple grating equation[13] with respect to order separation but the intensity distribution among diffraction orders is much more complicated.[18] A detailed treatment of the intensity in various orders as a function of the amplitude of the ultra-

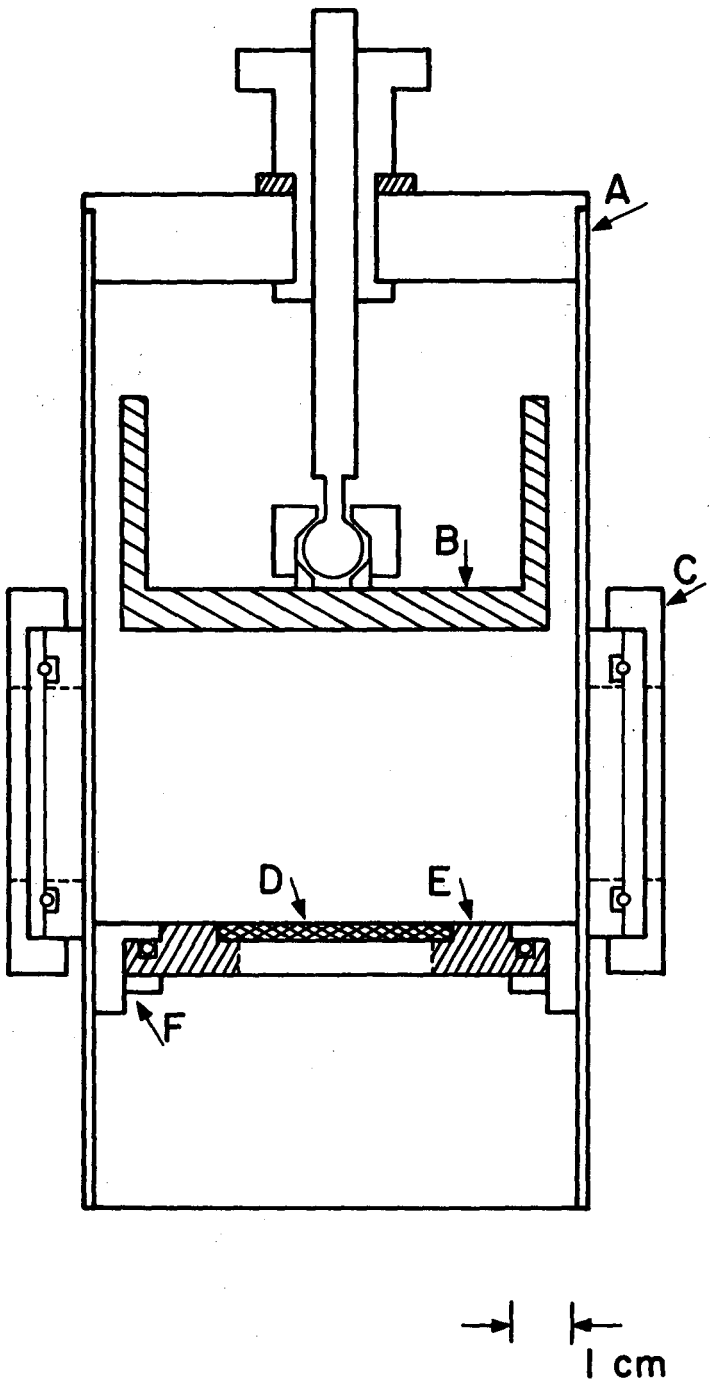

XBL 689-5937

Figure I-2

sonic wave, the pathlength through the ultrasonic grating region, and other parameters, has been given by Berry.[19] In practice it is only necessary to know that the intensity in various diffraction orders depends in a complicated way on the amplitude of the ultrasonic wave and to adjust the power to the crystal transducer for maximum modulation. The use of a water-ethanol mixture in the tank[16,20] in place of pure water has apparently greatly improved the temperature stability of the modulation;[15] it will now operate stably for several hours without adjustment.

The selection of the focal lengths of the lenses, particularly L_2 and L_3 in Fig. I-1, is dictated somewhat by the modulation frequency and the wavelength of exciting radiant energy. Lower modulation frequency and shorter exciting radiant energy wavelength result in smaller order separation in the diffraction pattern and a corresponding decrease in modulation and total optical transmission. Matched pairs of lenses having focal lengths of 140, 200 and 250 mm have been used for L_2 and L_3. The spacing and slit size of the multiple slits are also important in determining the modulating efficiency of the system. Those conditions outlined above which decrease order separation require smaller and more closely spaced slits. The multiple slits used for 5 MHz operation had 0.76 mm slits with 0.8 mm spacing and those used for 1 MHz operation had 0.38 mm slits with 0.41 mm spacing. The ultrasonic standing wave in the tank exists in a fairly well defined region above the transducer crystal. There is distortion of the wave near its edges at the interface with unaffected water-ethanol solution. The purpose of the aperture stop is to mask off this distorted region and thereby increase the uniformity of phase across the exciting beam. The size of the aperture again depends on many variables

but mainly on the size of the crystal tranducer in the tank. The diameter of the aperture stop is normally 15 to 20 mm. The quartz plate, which reflects a portion of the modulated beam onto the reference photomultiplier, must be placed so as to intercept the entire beam. The radiant energy sources, filters and samples used will be described below.

3. Electronics.

The crystaltransducer is driven by an exciter unit similar to that previously described by Berg.[14] Some changes in the oscillator part of the exciter were necessary to achieve satisfactory operation at 1.0 MHz, due to the low activity of quartz crystals in that frequency region. The variable output capability of the exciter is important in tuning the modulator.

The photomultipliers used, which are listed in Table I-A, were selected to give the best signal-to-noise ratio for the particular wavelength of interest. The wiring of the tube bases has been previously described in detail.[8]

The heterodyne stages are the same for both the reference and sample signals and, except for minor changes in tuned coupling circuits (see Appendix), are the same at both operating frequencies. The input signal from the photomultiplier at 5.206 or 1.000 MHz is beat with the signal from the corresponding local oscillator and the 1.000 kHz difference signal is amplified and used for phase shifting and detection. The heterodyne stage thus permits the use of much of the same electronic equipment at different modulation frequencies. The phase relation between the reference and sample signals at the modulation frequency is carried over to 1.0 kHz in the heterodyne stage.[12] The mixer tube

Table I-A

Summary of Experimental Parameters for Atomic Lifetime Measurements

Element	Wavelength in nm	Wavelength Isolation Filters	Photomultiplier	Range of $1 + \frac{L_f}{L_n}$ Free of Entrapment
Al	394.4	Interference filter 4.0 nm band pass	Amperex 56UVP	22
Al	309.3 308.2	Schott UG11 Corning No. 9-53	Amperex 56UVP	30
Ga	403.3 417.2	Wratten No. 39	RCA 7264	40
Ga	287.4 294.4	Nickel -Cobalt Sulphate Solution Corning No. 9-59	Amperex 56UVP	15
In	410.1 451.1	Corning No. 0-52 Wratten No. 39	Amperex 56UVP	50
In	325.6 325.9 303.9	Schott UG11	Amperex 56UVP	30
In	325.6 325.9	Schott UG11	RCA 7264	19
Tl	377.6	Wratten No. 39	RCA 7265	400
Tl	276.8	Nickel-Cobalt Sulfate Solution	Amperex 56UVP	12
Cu	324.7 327.4	Schott UG11	Amperex 56UVP	16
Ag	328.1 338.3	Schott UG11	RCA 7264	16
Ag	338.3	Schott UG11 Crown Glass lens	RCA 7264	7
Na	589.0 589.6	Interference filter 10.0 nm band pass	RCA 7264	60
Cs	455.5	Interference filter 4.0 nm band pass	RCA 7264	15
Pb	283.3	Nickel sulphate solution	Amperex 56UVP	50
Bi	306.8	Schott UG11	Amperex 56UVP	25
Hg	253.7	Nickel-Cobalt Sulphate Solution Chlorine gas	Amperex 56 UVP	12

can be a source of considerable noise and it was necessary to try a large number of tubes and select those with the best signal-to-noise characteristics.

At the time the equipment was modified for operation at 1.0 MHz it was thought that the heterodyne stage might be eliminated. There was, however, considerable difficulty, particularly in the phase shifters, due to non-linearity of components and due to small stray capacitances and inductances which are of considerable importance at high frequencies. In the end the heterodyne method was preserved.

The same local oscillator circuit is used at both frequencies with appropriate changes in the tuned circuits. The use of variable capacitance diodes in series with the crystal allows limited frequency variation[13] which is utilized to maintain the 1.0 kHz output from the mixers constant to within 0.1 Hz. This means that the modulation-frequency stability of the system rests in the transducer exciter unit. A counter is used to monitor the 1.0 kHz signal in the reference channel since any variation in this frequency will alter the behavior of the subsequent phase-shift circuits.

The analysis of the phase-shift circuit in previous work[13] is incomplete since the equivalent circuit used neglects the source impedance of the cathode followers which provide the signal to the series capacitor and resistor. The more complete equivalent circuit is shown in Fig. I-3. If the source impedance, R_s, is included in the calculation of the phase shift, θ then θ is given by

$$\theta = \tan^{-1} (R\omega C) + \tan^{-1} [(2R_s + R) \omega C]. \qquad (I-4)$$

This solution becomes identical to Stafford's[13] result when $R_s = 0$.

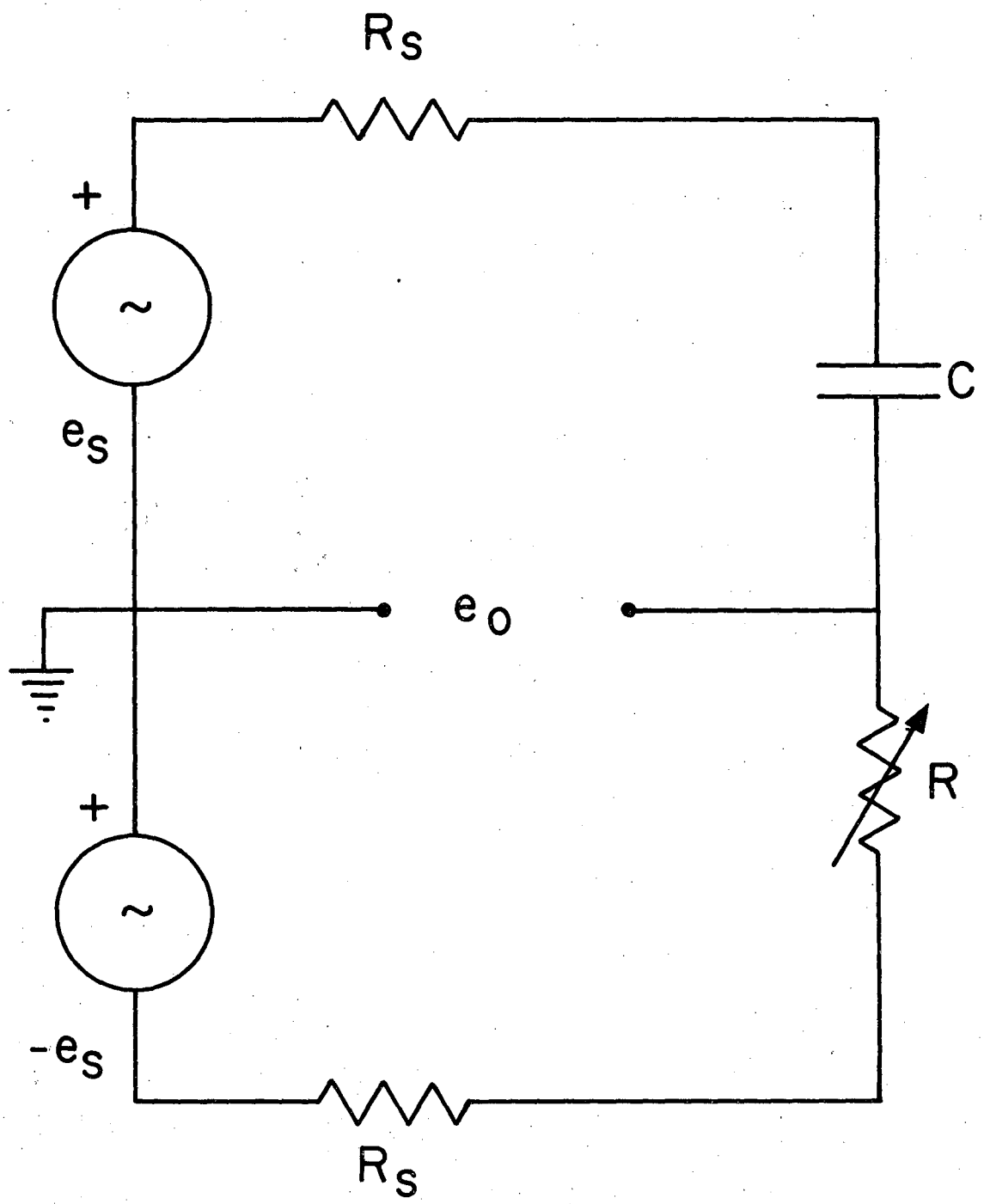

XBL 689-5939

Figure I-3

Figure I-4 shows the difference in phase-shift calculated assuming R_s is zero and the actual phase-shift for an R_s of 200 or 300 ohms. It is assumed in these data that the sample shifter was initially at minimum shift corresponding to an R of zero ohms, which is the usual experimental procedure. The lower abscissa gives value of R while the upper abscissa gives the corresponding phase-shift for an R_s of zero. It is seen from Fig. I-4 that errors of about one degree can occur by neglecting the effect of R_s resulting in an error of about 4% in the lifetime. It should be emphasized that Fig. I-4 does not show the error in the absolute phase-shift produced by the circuit shown in Fig. I-3 which will be greater for smaller values of R as indicated in Eq. (I-4). However, recalling that a phase-shift measurement is the result of the difference between two absolute phase determinations, the error will be small for small measured shifts since the large error in the absolute shifts will be nearly the same and will cancel.

The phase null detector has been discussed in detail by Chutjian[8] and he has corrected misconceptions concerning its operation which have appeared in earlier works.[13] In addition, Chutjian has described the various checks which can be made on the operation of the phase shifters and phase-null detector to show up any malfunction. A dual beam scope and chart recorder are used to monitor the signals going into the detector and provide a display from which a qualitiative feel for the data may be obtained.

The overall performance of the equipment can be calibrated by measurement of the time of flight of light over carefully measured distances. This was done for several distances ranging from a few meters up

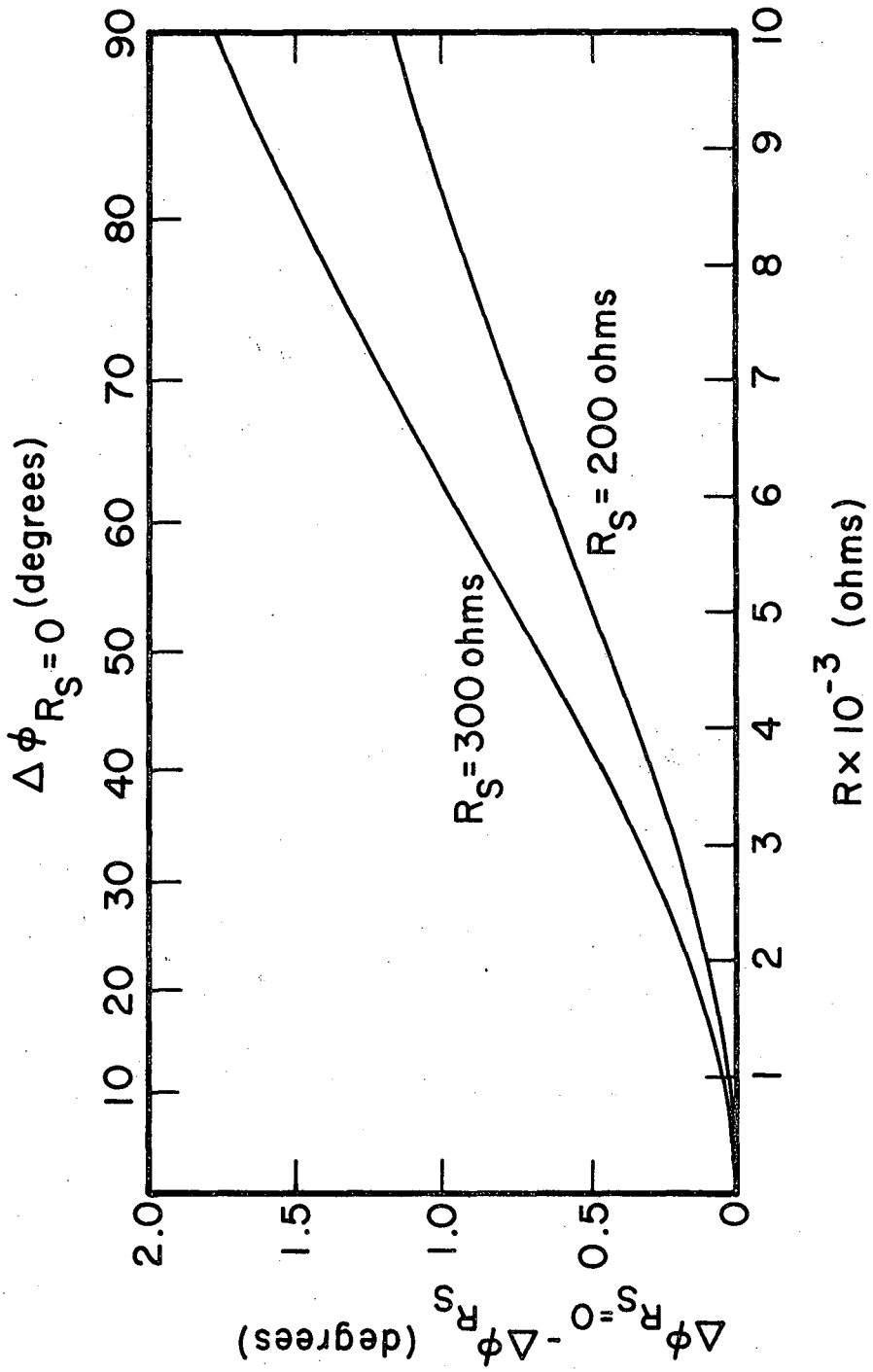

XBL 689-5938

Figure I-4

to eight meters during 5.2 MHz operation and for up to 30 meters during 1.0 MHz operation. The agreement between calculated and measured phase shifts was never worse than 1%, even when the effect of R_s was neglected. When the value of R_s, which was obtained by direct measurement, was included the agreement was better than 0.1%. The value of R_s used in this work was 215 ohms but might be expected to vary slightly with age of the electron tube as well as for different tubes.

4. Sample Containment.

With the exception of Hg and Cs, all of the lifetimes reported here were measured while the metal atoms were in an atomic beam. A diagram of the beam chamber is shown in Fig. I-5. Beam were produced by effusion through 1.5 mm orifices in crucibles which were heated by 0.05 mm tantalum-foil-resistance heating elements. Graphite crucibles were used for Ga, In, Tl, Cu, Ag, Pb, and Bi while quartz was used for Na and alumina for Al. There was some difficulty obtaining a stable Al beam as the aluminum in the crucible had a tendency to bump, thereby wetting the outside of the crucible and destroying the heating element. The introduction of a small amount of graphite into the crucible apparently eliminated the formation of an aluminum oxide film on the aluminum surface in the crucible and resulted in a steady beam. The density of the atomic beams was easily controlled by adjusting the heating power. A residual gas pressure of about 5×10^{-5} Torr was maintained in the beam chamber.

During the course of several Ag runs a marked sluggishness in the variation of fluorescence radiance with change in furnace heating power was observed. This was attributed to the melting or solidifying of Ag

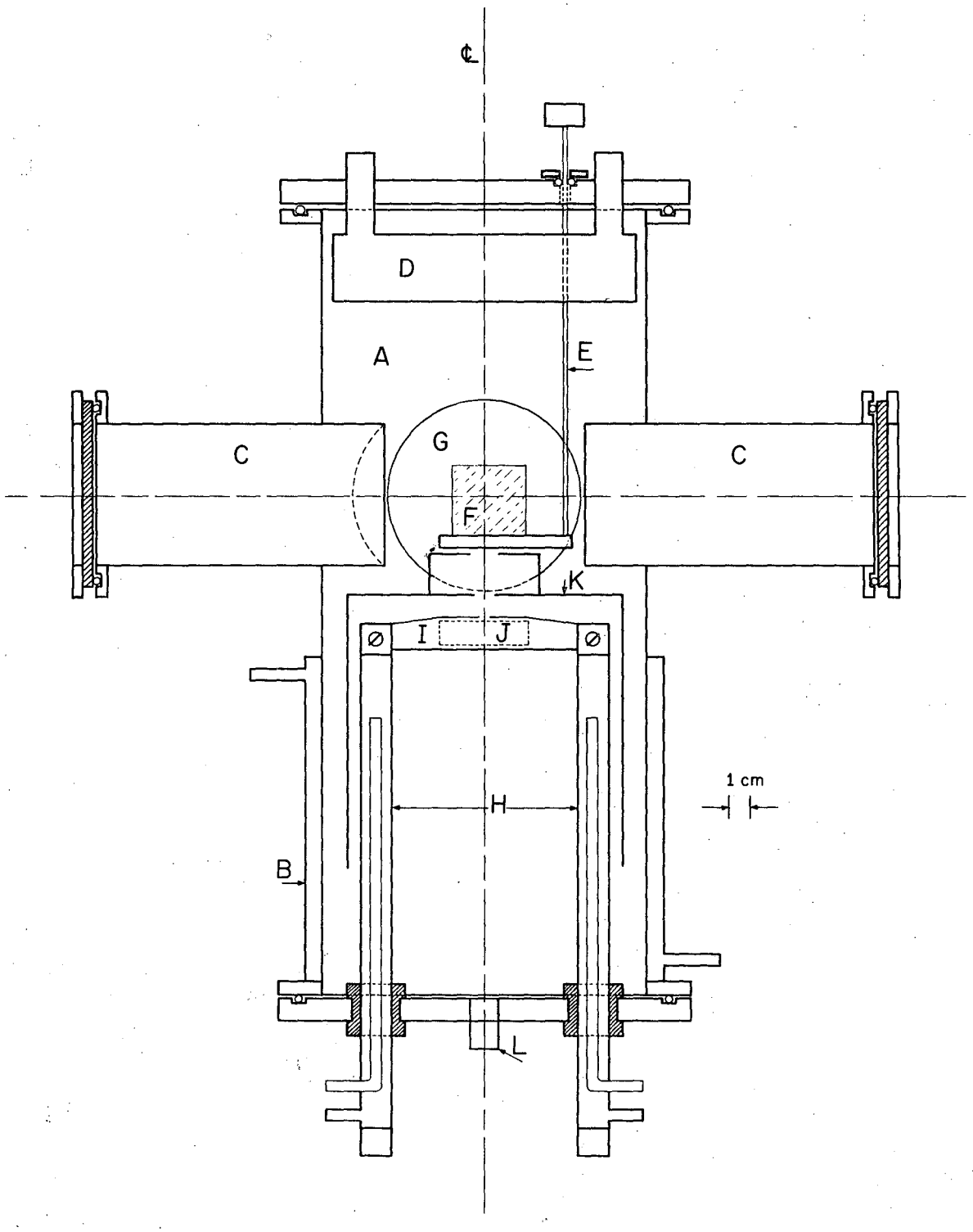

XBL 689-5941

Figure I-5

metal in the crucible. The vapor pressure of Ag at its melting point is about 0.003 Torr[21] corresponding to a beam density of 1.2×10^6 per mm^3. Assuming the fluorescence radiance to be proportional to the Ag beam density, it was concluded that a typical run went from crucible pressures of about 2.5×10^{-4} Torr (limit of detectability of fluorescence) to roughly 1.5×10^{-2} Torr (beginning of entrapment of resonance radiant energy the beam.) At the position in the beam where excitation occurs, this corresponds to a range of Ag atom density in the beam of from about 10^5 to 6×10^6 per mm^3. These numbers, when scaled by appropriate f-value and Doppler width ratios, should be typical of all the metals studied. It should be noted that, because of the decrease in randomness of motion and resulting decrease in Doppler width, the mean free path of a photon emitted in an atomic beam, with a total opening angle of 40° and a direction of photon travel perpendicular to both the mean motion of the beam and the exciting radiant energy, will be about ten times less than in the atomic gas at thermal equilibrium at the same temperature and density.

Cesium was contained in a heated Pyrex cell which has been previously described.[16] Hg was contained in a quartz cell which was constructed with Wood's horns opposite both the entrance window for the exciting radiant energy and the viewing window for the fluorescence. A similar cell is shown in Fig. 18 of reference 14. The vapor concentration within the cells was controlled by the temperature of a side arm but the control was not as good as might be hoped. In both cases it was necessary to heat the body of the cell for some time, while the sidearm was maintained at liquid nitrogen temperature, in order to condense the metal into the side arm. Data were then taken with the body of the cell at room temperature, or slightly above in the case of Cs, while the side arm was slowly warmed.

As will be discussed in depth below, it is necessary to minimize and control scattered exciting radiant energy; as well as radiant energy emitted from the heating element in the case of a beam sample. This was accomplished by having the entrance and exit windows of the beam chamber set back in 105 mm deep side arms and through the use of baffles around the crucible and sample photomultiplier.

It has been repeatedly stressed in previous work[8,14] that the phase of the exciting radiant energy is not constant across the exciting beam. Because of this, it is necessary that the sample, and the means used to scatter the exciting beam for measurement of the exciting radiant energy phase, intercept the exciting beam in the same way. For closed cells, as in the case of Hg and Cs, this is accomplished by using dilute scattering sols in cells of the same geometry as the sample cell.[8,16] Where the sample is in an atomic beam, the exciting radiant energy is scattered from a ground glass plate which is attached to the top of a beam shutter and can be swung into the path of the exciting radiant energy directly over the crucible orifice. To insure that this procedure correctly sampled the exciting phase, a check was made before and after each run by comparing the phase of scattered radiant energy from the glass plate and from a scattering sol placed in the beam chamber. It was found that after some runs, a thin deposit of metal had formed on the frosted glass and altered its scattering properties so that the two procedures did not agree. Careful cleaning of the frosted glass always restored the agreement. The validity of using the glass plate is further supported by the close agreement between the lifetime of Na measured in a closed cell[16] and in the beam.

5. Excitation Sources.

In exciting atoms in a beam, it is important that the source produce strong lines that are not self-reversed. Because of the narrow Doppler width of atoms in the beam, strongly self-reversed lines may fill to excite the sample while even slight self reversal will increase the level of unusable radiant energy and decrease the signal-to-scattered radiant energy ratio. Considerable time was spent trying to develop the most effective resonance lamps. In the end, all of the lamps, except for Na and Al, were of the electrodeless discharge type. They were constructed of well out-gased quartz tubing 8 mm O.D., 6 mm, I.D., about 50 mm long. Excitation was by microwaves at 2,450 MHz produced by a commerical diathermy unit and using a type A antenna.

A simple heater was used for the Cu, Ag, Tl, Bi and Pb lamps. The lamp slipped smoothly into a piece of 9 mm I.D. quartz wrapped uniformly with No. 28 Nichrome wire. The lamp and heater were then fitted inside at 18 mm I.D. outer quartz jacket to reduce convection currents and improve the heating efficiency.

The Cu, Ag, and Bi lamps contained a small amount of distilled iodide of the element and about 1 Torr of Argon. In, Ga and Pb iodide lamps made in the above manner were unstable and showed severe self-reversal of the strong resonance lines. This is because the In, Ga and Pb iodides are sufficiently volatile that the heating of the lamp by the microwave power causes a high density of halide vapor which leads to a high density of electrons. This causes instability and a high density of atoms leading to self reversal of the resonance lines. The Tl lamp contained a small amount of distilled Tl and about 1 Torr of Argon.

This was found to work better than a halide lamp.

The following procedure was developed to allow introduction of such a small amount of In, Ga and Pb iodide into the lamp that it could completely vaporize without interfering with the stability and useful radiance of the lamp. A small piece of metal (undistilled) was placed in the unsealed lamp. Iodine in contact with a temperature bath provided 0.03 Torr of I_2 pressure (about 2.2×10^{-9} moles) in the case of In and Ga and 0.22 Torr for Pb. One Torr of argon was added and the lamp sealed off. The metal was left undistilled so that no appreciable formation of iodide would occur before the lamp was sealed off an thus the total amount of iodide formed in the lamp was closely controlled. Excitation with microwaves and mild heating then caused the formation of the iodide. The Pb lamp ran best with slight heating, the In lamp with no heating, and the Ga lamp with air cooling. A properly operating lamp was characterized by a marked weakening or disappearance of the molecular iodide and argon features with respect to the atomic emission lines.

For Na a commercial Osram lamp was found to be satisfactory. It was run from a square wave generator to minimize low freqency ripple. A germacidal Hg lamp excited by microwaves and air cooled at its base was used for Hg excitation. The Cs was supplied in 0.25 gm ampules by the Kawecki Chemical Co., Revere, Pennsylvania. Microwave excitation of these ampules made the best Cs lamp. Slight heating was necessary to start the lamp but after it lit, air cooling of the lower portion of the ampule was necessary. In all cases the microwave power level and the amount of heating or cooling of the lamp was adjusted until maximum fluorescence was produced at constant atomic beam density or cell concentration.

The atomic beam had a total opening angle of about 40 degrees so that the effective Doppler width was about 1/3 of that of atoms in thermal equilibrium at the crucible temperature. Thus maximizing the fluorescence radiance meant that the lamps were emitting reasonably sharp unself-reversed lines. Tests made with Tl using the 377.6 nm line and Cu using the unresolved 324.7 and 327.4 nm lines showed that atomic beams of high densities, corresponding to severe entrapment, could absorb up to 1/3 of the exciting resonance lines.

Several lamp designs were tried for Al. The most satisfactory of these was a flow lamp inspired by the lamps of Budick et al.[22] A diagram of the lamp is shown in Fig. I-6. In operation a discharge was started in the necked down portion of the lamp with the helium pressure at about 1 Torr. An air cooled microwave cavity, similar to the type 5 cavity described by Broida et al.,[23] powered by the 2,450 MHz diathermy unit maintained the discharge. The molybdenum crucible containing anhydrous aluminum chloride was then slowly warmed to the point where the chloride just vaporized and the discharge was taken over by the aluminum. At this point the performance of the lamp, as determined by fluorescence radiance from the beam, was quite insensitive to changes in helium pressure in the range from 0.1 to 10 Torr and to microwave power. Increased heating of the aluminum chloride, however, resulted in a drop in fluorescence radiance. The lamp would operate stably for several hours. The life of the lamp could probably be lengthened considerably if an effort was made to eliminate water from the system. Water reacts with the aluminum chloride and forms aluminum hydroxide which plugs the crucible openings.

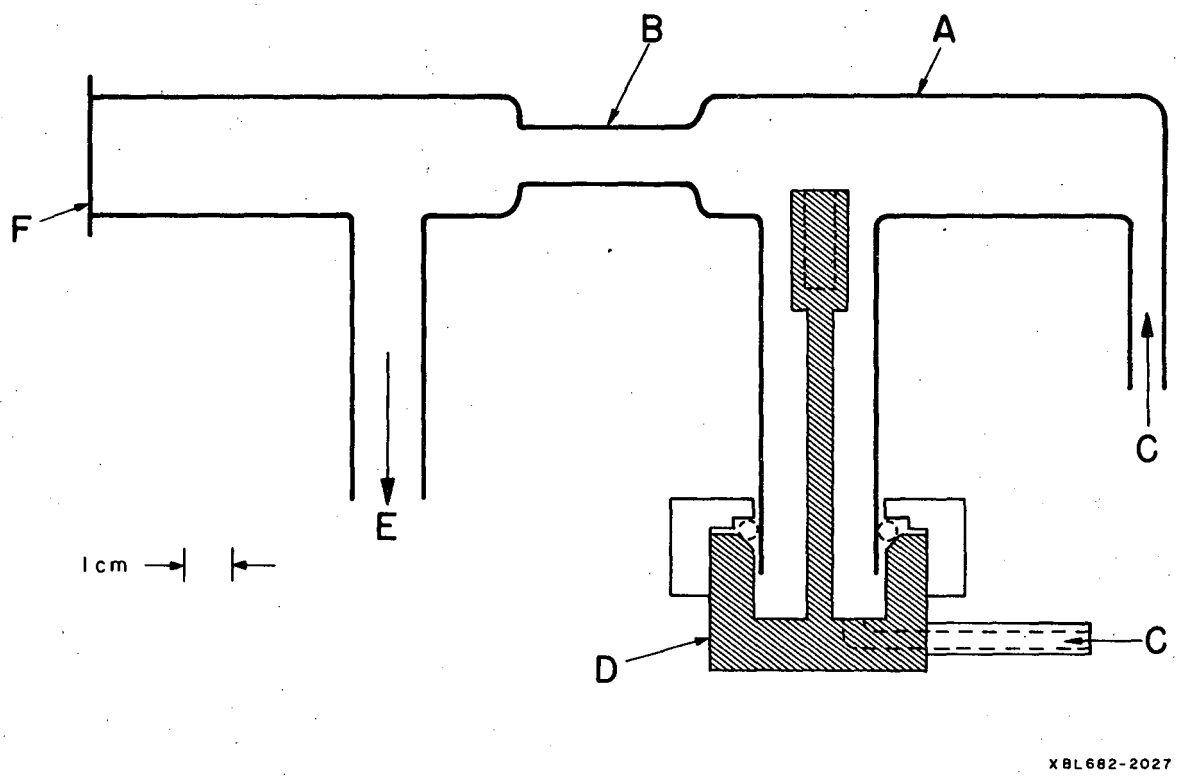

Figure I-6

C. Analysis and Results

1. General Discussion.

Each measurement of $\Delta\phi$, that is the difference in phase between the exciting radiant energy and the fluorescence radiant energy, is a measure of the lifetime of the excited state being studied under the experimental conditions existing at the time of the measurement. There are three important processes, aside from possible systematic experimental errors, which might cause this measured lifetime to be different from the radiative lifetime of the state; quenching of the excited state through collisions with other atoms or residual gas molecules, scattered exciting radiant energy striking the photocathode of the sample photomultiplier along with fluorescence radiant energy, and radiation entrapment where the photons emitted by atoms excited by the exciting radiant energy are in turn absorbed so that the radiant energy reaching the sample photomultiplier is composed of an appreciable fraction of secondary fluorescence radiance.

The first of these processes, excited state quenching, is not a problem in the work described here because of the very short lifetimes studied and the low particle density of the sample. This is certainly not always the case as is seen from work on species of longer lifetime or at greater density.[8,24] The entrapment process is very difficult to evaluate in a quantitative way for experiments of the type recorded here, since it depends not only on the f-value of the transition and the particle density, but also on the detailed nature of the exciting radiant energy, fine structure of the radiant energy being entrapped, and the degree of branching from the excited state involved. Kibble, Copley and Krause[25] have

investigated the effects of radiation entrapment for the sodium D lines and have shown that the theoretical treatment of Milne[26] is closely followed over a wide range of sodium density. In the work reported here data could be taken at vapor densities which were low enough to make the effects of radiation entrapment negligible.

The problem of scattered exciting radiant energy, on the other hand, is very important in studying resonance transitions and can be treated exactly. This was first done by Rosenblatt[27] and by Berg.[14] The problem has also been discussed in detail by Chutjian.[8] The radiant energy detected by the sample photomultiplier is composed of two parts, the fluorescence, which contains the phase shift information due to the radiative lifetime of the sample, and the scattered exciting radiant energy, which may have a complicated phase relation with the direct exciting beam. This can be represented by the relation

$$L_m \cos(\omega t - \phi_m) = L_f \cos(\omega t - \phi_f) + L_n \cos(\omega t - \phi_n) \qquad \text{(I-5)}$$

where L_m, L_f and L_n are the measured, fluorescence, and scattered radiances respectively and ϕ_m, ϕ_f and ϕ_n the corresponding phases. When it is assumed that ϕ_n is unshifted from the exciting beam, which is experimentally observed to be so in almost all cases, it can be shown by rearrangement of Eq. (I-5) and introducing the relation given in Eq. (I-3) that

$$\tau_K = \tau_k^\circ \left[1 - \frac{1}{\dfrac{L_f}{L_n (1 + \omega^2 \tau_k^2)^{1/2}} + 1} \right]. \qquad \text{(I-6)}$$

This equation shows that the measured lifetime, τ_k, is a function of the radiative lifetime, τ_k° and the ratio L_f/L_n. A plot of τ_k versus log $(1 + L_f/L_n)$ gives a smooth curve, of the type shown in Figs. I-7 and I-8, which approaches τ_k° for large values of L_f.

Figure I-9 shows the atomic energy levels of interest for each of the elements studied. Figures I-7 and I-8 show, respectively, the data taken on the two systems which represent the largest and smallest range of $(1 + L_f/L_n)$ corresponding to vapor densities for which radiation entrapment is not a problem. Table I-A lists the elements studied together with the wavelengths of the radiant energy observed, the isolation filters and photomultipliers used, and the range of $(1 + L_f/L_n)$ over which lifetimes could be measured before the onset of more than 2% lengthening in measured lifetime due to radiation entrapment. Table I-B lists the lifetimes measured in this work along with their estimated possible errors. The possible errors are the sum of a 0.1 nsec systematic uncertainty and the uncertainty in fitting the experimental data to the theoretical curve given by Eq. (I-6).

It seems best at this point to consider each atom seperately in analyzing the experimental observations and in discussing the problems encountered and assumptions made in converting the raw data into the lifetimes listed in Table I-B.

2. Aluminum.

At the temperatures necessary to produce the aluminum beam the relative populations of the $^2P_{1/2}$ and $^2P_{3/2}$ states are nearly those of their statistical weights (2 and 4) since they are separated by only 0.01 eV. It was possible to excite the $^2S_{1/2}$ state using an interference

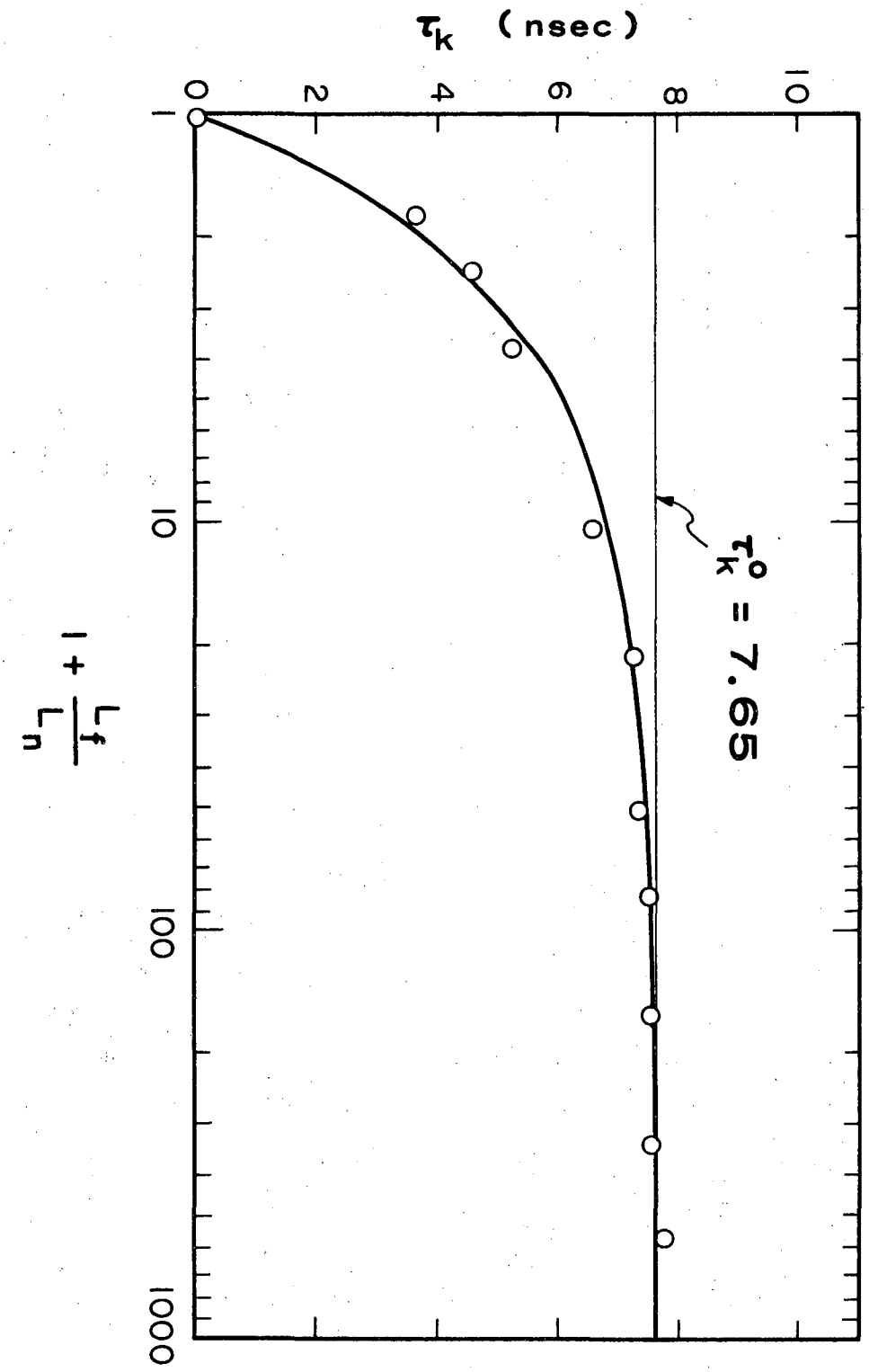

XBL 672-870

Figure I-7

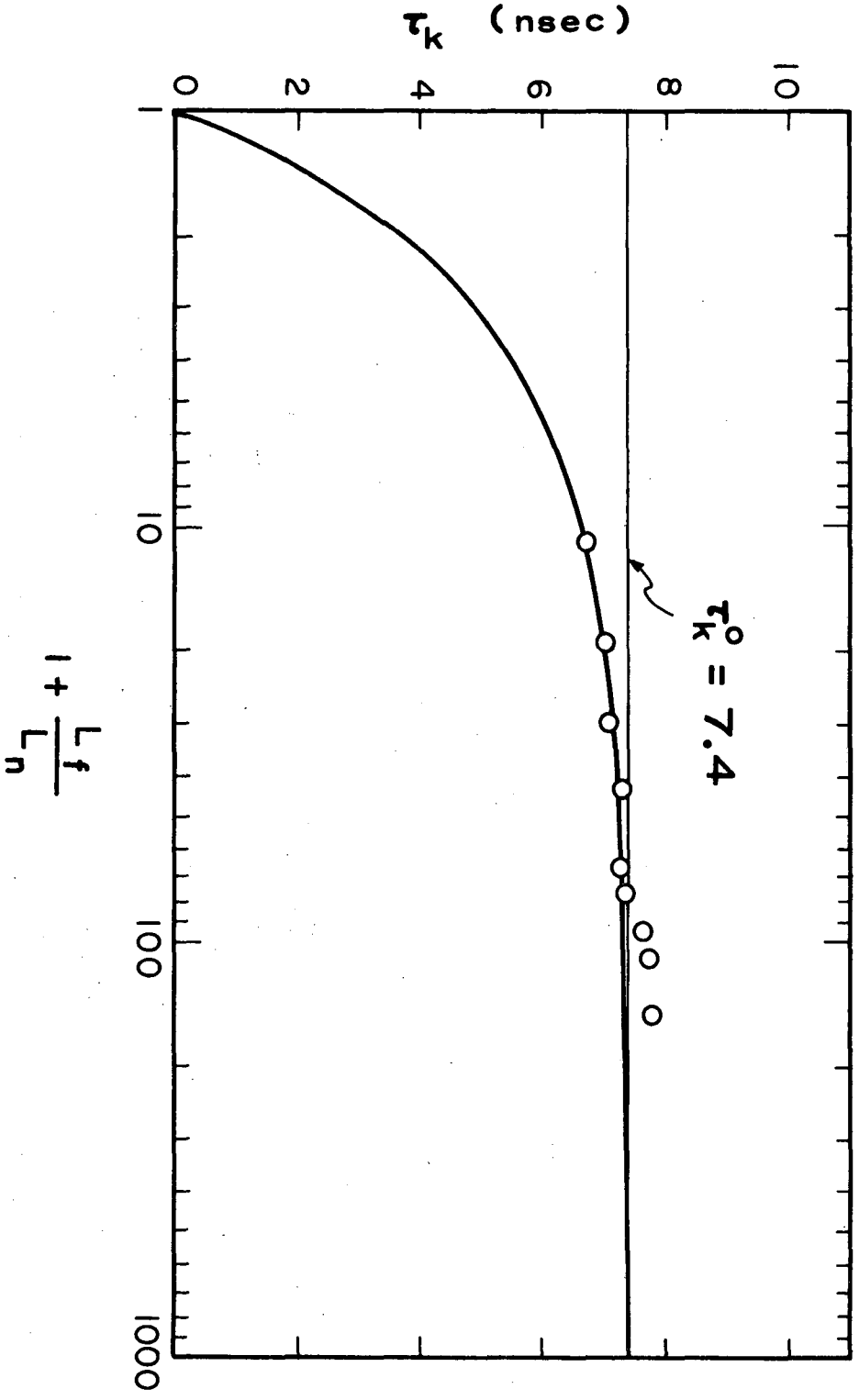

XBL 672-871

Figure I-8

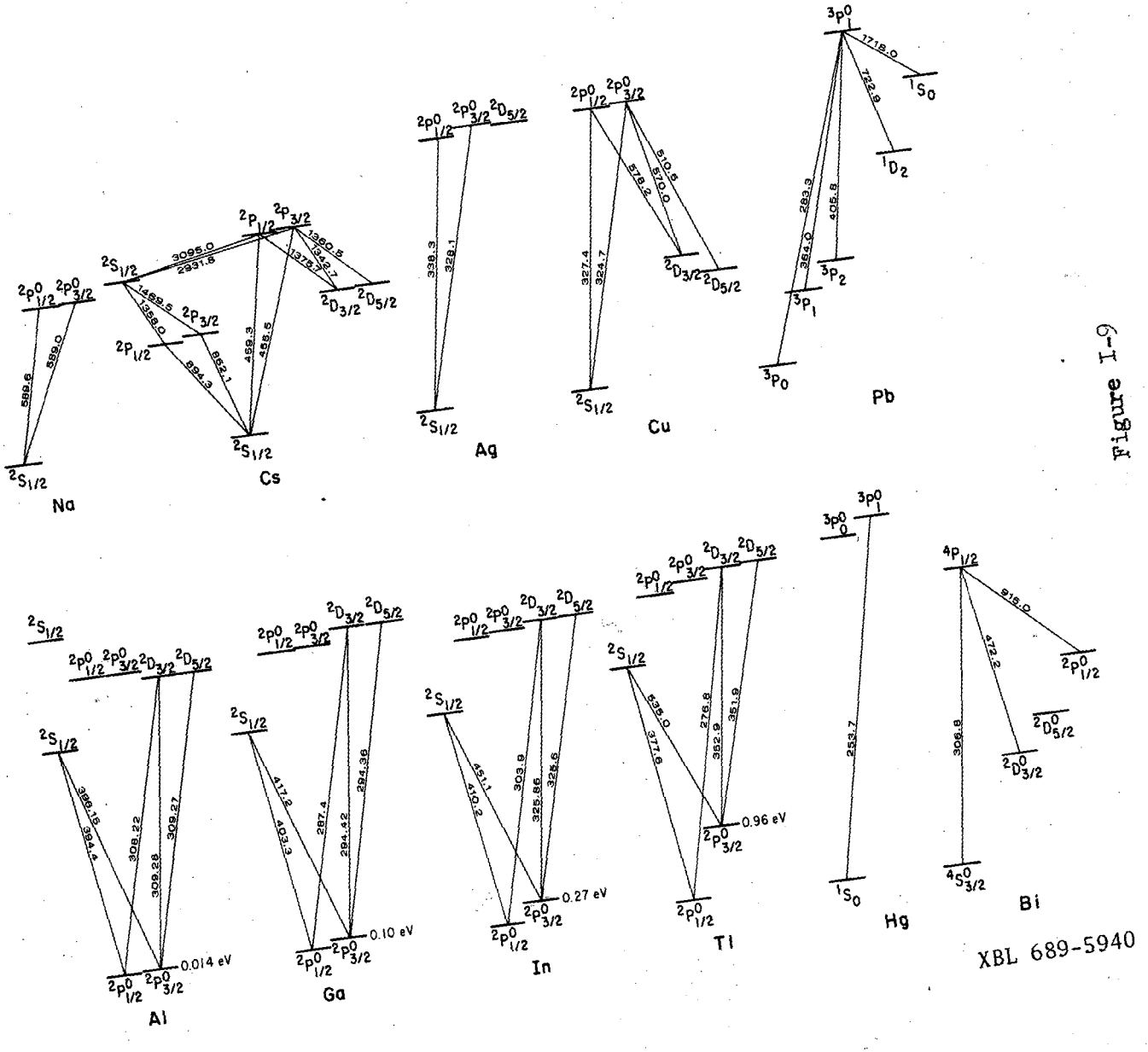

Figure I-6

XBL 689-5940

TABLE I-B

Measured Lifetimes

Element	State	Lifetime (nsec)
Al	$4s^2S_{1/2}$	7.05 ± 0.3
	$3d^2D$	13.7 ± 0.4
Ga	$5s^2S_{1/2}$	7.6 ± 0.4
	$4d^2D$	7.7 ± 0.3*
In	$6s^2S_{1/2}$	7.5 ± 0.3
	$5d^2D_{3/2}$	7.9 ± 0.5
	$5d^2D_{5/2}$	7.9 ± 0.5
Tl	$7s^2S_{1/2}$	7.65± 0.2
	$6d^2D_{3/2}$	6.9 ± 0.4
Cu	$4p^2P^o$	7.2 ± 0.3
Ag	$5p^2P^o_{1/2}$	7.5 ± 0.4
	$5p^2P^o_{3/2}$	6.7 ± 0.4
Na	$3p^2P^o$	16.2 ± 0.3
Cs	$7p^2P^o_{3/2}$	114.0 ± 4.0
Hg	$6p^3P^o_1$	115.0 ± 3.0
Pb	$7s^3P^o_1$	6.05 ± 0.3
Bi	$7s^4P_{1/2}$	5.9 ± 0.2

* = $1/2(\tau^2D_{3/2} + \tau^2D_{5/2})$

filter centered on 394.4 nm which assured no excitation of other states.

With the lamp operating under normal conditions, the emitted $3d\,^2D$-$3p\,^2P$ multiplet was examined under high resolution and these lines were found to be self-reversed. There was, however, sufficient radiant energy to excite fluorescence in the atomic beam over the density range necessary for the evaluation of the effects that scattered exciting radiant energy and radiation entrapment have on the measured lifetime. At high beam densities, corresponding to severe entrapment, up to 5% of the total exciting radiant energy could be abosrbed. Placing a filter cell containing a $NiSO_4$-$CoSO_4$ solution, which is transparent only between 330 and 230nm, in front of the sample photomultiplier produced no change in the measured lifetime of the $3d\,^2D$ state indicating that the $4s\,^2S$ state was not excited. This observation is also evidence against interference by molecular species such as Al_2O, which are no doubt present in the beam, and which might interfere with atomic measurements.

3. Gallium.

The $^2P_{3/2}$ state lies only 0.10 eV above the $^2P_{1/2}$ ground state. At the temperatures used to produce the Ga atomic beam both states were about equally populated. Relative radiance measurements of the fluorescent radiation at 287.4 nm and 294.4 nm indicated that the measured lifetime was an equally weighted average of the lifetimes of the $^2D_{3/2}$ and $^2D_{5/2}$ states. The wavelength composition of the exciting radiant energy and the fluorescent radiant energy was roughly the same during measurement of both $^2S_{1/2}$ and ^2D state lifetimes. Measurement of the ^2D state lifetime with and without a Corning No. 9-53 cut-off filter in the exciting beam produced no change in lifetime thus indicating that the presence of

radiant energy of wavelength shorter than 280 nm, which could excite the $6s\ ^2S_{1/2}$ state, was not a problem.

4. Indium.

The $^2P_{3/2}$ state lies only 0.2 eV above the ground state and therefore has a population of about 15% that of the ground state at the temperatures needed to produce the atomic beam. This means that the $^2D_{5/2}$ state is being excited as well as the $^2D_{3/2}$ state when only a Schott UG-11 wavelength selection filter is used. However the S-11 spectral response of the RCA 7264 photomultiplier tube falls sharply between 325.6 nm and 303.9 nm. It was found that the measured ratio of fluorescent radiance at 303.9 nm to that at 325.6 and 325.9 nm was 1/8 using the 7264 tube while it was 1/0.8 using an Amperex 56UVP with its U spectral response. The relative radiance measurements were made using a 1/4 meter Farrand Ultra-Violet-Visible Grating Monochrometer with a 10 nm band pass. The same phase-shift was obtained with both photomultiplier tubes indicating that the lifetimes of the $^2D_{3/2}$ and $^2D_{5/2}$ states are equal.

In the case of the $^2S_{1/2}$ state both the fluorescent and exciting radiances had the same flux ratio for $L_{451.1}/L_{410.1}$ so there was no problem from the wavelength effect on photomultiplier transit time such as that discussed below in the case of thallium. Using an interference filter to eliminate 451.1 nm from the exciting radiant energy while viewing about an equal mixture of 410.1 and 451.1 nm radiant energy in fluorescence with an Amperex 56UVP, caused at most a 0.1 nsec lengthening of the observed lifetime. The wavelength effect decreases markedly with increasing photon energy and was not a problem while making measurements on the ^2D states.

5. Thallium

The Tl and argon electrodeless discharge lamp emitted at least ten times more fluorescence producing radiant energy at 276.7 nm than a Tl Osram lamp with a special quartz jacket.

While studying the $^2S_{1/2}$ state lifetime with a 7265 photomultiplier a lengthening in measured lifetime of the order on one nsec was observed when the fluorescence was viewed at 535.0 nm instead of at the excitation wavelength 377.6 nm. The effect was attributed to a variation in electron transit time between the photocathode and the first dynode for different incident photon energies as reported by Muller et al.[28] As expected, the transit time difference was found to be proportional to the reciprocal of the photocathode-to-first-dynode voltage.

6. Copper.

A branching ratio of 0.985 for both $^2P_{3/2} - {}^2S_{1/2}$ and $^2P_{1/2} - {}^2S_{1/2}$ transitions was computed using an average of the results of Riemann[29] and of Corliss and Bozman.[2] The hook method relative f-values for the two transitions obtained by Ostrovskii and Penkin[30] then predict equality of the two upper state lifetimes to within experimental uncertainties. Therefore no attempt was made to separate the two resonance lines during the lifetime measurements.

7. Silver.

The fluorescence radiance ratio seen by the RCA 7264 tube through a Schott UB-11 filter was $L_{338.3}/L_{328.1} = 2/3$ when the lamp was set to produce maximum fluorescence. A lifetime measured under these conditions was then resolved in the following way: $0.4\,\tau\,{}^2P_{1/2} + 0.6\,\tau\,{}^2P_{3/2} =$

7.0 nsec. A crown glass lens was found which transmitted 338.3 nm but attenuated 328.1 nm quite strongly. With this lens in the system a lifetime was measured which was determined to be $0.9\ \tau\ ^2P_{1/2} + 0.1\ \tau\ ^2P_{3/2} = 7.4$ nsec. The two equations yield a lifetime of 6.7 nsec for the $^2P_{3/2}$ state and 7.5 nsec for the $^2P_{1/2}$ state.

8. Sodium.

No attempt was made to separate the two D-lines since the relative f-values of previous work (see discussion of Na below) indicate that the lifetimes of the $^2P_{1/2}$ and $^2P_{3/2}$ states are equal.

9. Lead.

The 283.3 nm line was observed in fluorescence over an entrapment free range of $(1 + L_f/L_n)$ of 50. Since the branching ratio for the 283.3 nm line is only 0.27,[31] only about 1/3 of the fluorescent photons were used.

10. Bismuth.

Useful Bi beams were produced at crucible temperatures of around 900 K. At this temperature about 40% of the beam was Bi_2 molecules.[21] The Bismuth iodide resonance lamp did not emit any detectable Bi_2 features and there are no Bi_2 lines in the vicinity of the 307.8 nm atomic Bi resonance line so the presence of Bi_2 molecules in the beam had no effect on the atomic lifetime measurements.

11. Mercury.

Mercury was the first element to be measured using the 1 MHz modulation. The lifetime of the $^3P_1$ state has been the subject of consider-

able work and is presumably well known. It was, for this reason, selected to check the operation of the 1 MHz system. The isolation of the 253.7 nm line provided by a $NiSO_4$ - $CoSO_4$ solution filter was found to be inadequate. Longer wavelength radiant energy, particularly the 313.0 nm doublet, contributed greatly to the scatter and was not of the same phase as the 253.7 nm exciting line. This was attributed to the fact that to obtain sufficient modulation at 1 MHz it is necessary to use longer focal length lenses on the ultrasonic tank which enhances the effect of chromatic abberation. The addition of a chlorine gas filter and the use of a double Wood's horn cell reduced scattered radiant energy so that sufficient data could be taken in the entrapment free vapor density region to fit the theoretical curve. It is believed that a filter for the 253.7 nm line with greater transmission than the 15% achieved with the filter used here would permit the probable error in this measurement to be reduced. Nevertheless, the agreement between this work and that of previous measurements is encouraging and indicates no serious systematic problem at 1 MHz operation.

12. Cesium.

The $^2P_{3/2}$ state of Cs was excited using an interference filter with a full width at half-maximum-transmission of 1.9 nm and centered on 455.7 nm, which completely blocked the 459.3 nm line.[6] No change was observed in the measured lifetime when a Wratten number 48 filter was placed in front of the sample photomultiplier indicating that radiation into the ^2S or ^2D states, which lie below the $^2P_{3/2}$ state, and which would eventually come out in the main resonance lines at 852.1 and 894.3 nm could not be detected by the RCA 7264 sample photomultiplier with its S-11 response.

D. Discussion

1. Introduction

The determination of f-values from the lifetime data presented in Table I-B requires that the relative transition probabilities for all transitions depopulating the excited state be known. For most of the atoms studied here there has been a great deal of previous work determining these relative transition probabilities. The notation used in the literature is by now means uniform and each paper must be read carefully to insure understanding. There are numerous cases where authors have incorrectly compared their work to that of others because of misunderstanding.

The problem is to evaluate these data and select that which is most reliable. In the discussion below each atom studied is considered separately. The previous work judged most reliable together with the present results and a recommended best value are presented in tabular form for all transitions involved. The values of Corliss and Bozmann[2] have been included in each table for easy comparison, since they are probably the most widely distributed.

2. Aluminum

The earliest reported[32] experimental work on aluminum transitions is that of Voorhoeve[33] who obtained a value of 0.99±0.15 for the ratio $f_{394.4}/f_{396.2}$ and 0.96±0.15 for $f_{309.3}/f_{308.2}$ from arc emission. Kunisz[34] using the same technique obtained 1.2±0.03 and 0.83±0.03 for these ratios and indicated that Voorhoeve may have had difficulties due to reabsorption. This seems unlikely in the light of later work. Korolev and Kvaratskheli[35] have measured the relative radiance from a plasmatron and obtained 1.05 for $f_{394.4}/f_{396.2}$.

The hook method was first used for aluminum by Parchevskii and Penkin[36,37] to get 1.03 for $f_{394.4}/f_{396.2}$. Several measurements by the hook method[38-41] have all determined this ratio to be 1.00 within experimental error. Ostrovskii[39] and Penkin and Shabanova[40,41] have used the hook method to determine $f_{309.3}/f_{308.2} = 1.03 \pm 0.06$ as well as $f_{308.2}/f_{394.4} = 1.49 \pm 0.05$.

Allen and Asaad[42] used emission from dilute copper alloys to make absolute measurements of aluminum f-values but indicated their results were very uncertain due to inaccuracy in the measured aluminum content of the alloy. Their values are $f_{394.4} = 0.016$ and $f_{396.2} = 0.013$; these were later revised and increased by a factor of 1.5. Addink[43] who was attempting to correlate the reliability of spectral lines for use in spectrographic quantitative analysis with the lifetime of the excited state, estimated $f_{396.2}$ to be 0.06 from the radiance of the line in an arc.

A number of calculations have been made to determine f-values for transitions of aluminum. Biermann and Lübeck[44] have calculated the total f-value for the 3^2P-4^2S transition to be 0.13 and for the 3^2P-3^2D transition to be 0.91 using the Hartree method. The Coulomb approximation of Bates and Damgaard[45] gives 0.051 and 0.63 for these transitions. More recently, Synek and Lichodziejewski[46] have obtained $f_{(3^2P-4^2S)} = 0.25$ and $f_{(3^2P-3^2D)} = 0.83$ using the Hartree-Fock method with the dipole length operator. Hanus[47] has calculated the relative f-values for the lines of the 3^2P-4^2S and 3^2P-3^2D multiplets for first order perturbation caused by spin orbit interaction and found $f_{394.4}/f_{396.2} = 1.02$; $f_{309.3}/f_{308.2} = 0.99$. Gruzdev[48] has made calculations for several transitions which seem to agree with experimental results for the sharp series but not for the diffuse series.

The lifetime of the $4^2S_{1/2}$ state has been measured previously by Demtröder[20,49] who got a value of 6.43±0.12 nsec compared to the value 7.05±0.3 nsec obtained in this work. Demtröder[20] then used the $4^2S_{1/2}$ lifetime to normalize relative f-values which he obtained from absorption measurements in an aluminum beam. By this method he obtained $f_{(3^2P-3^2D)} = 0.28$. Budick[50] has measured the lifetime of the $3^2D_{5/2}$ state by the level crossing method and obtained 13.6±1.4 nsec, in good agreement with the 13.7±0.4 nsec obtained in this work.

The f-values based on the lifetimes measured in this work are listed in column 7 of Table I-C. In calculating these values it was assumed that $f_{394.4} = f_{396.1}$ and that $\tau 3^2D_{3/2} = \tau 3^2D_{5/2}$. These assumptions are based on the relative f-value results discussed above and the lifetime measurement of Budick and are expected to be valid for Russell-Saunders coupling. The selected values listed in Table I-C are those measurements in the literature considered most reliable. The recommended f-values in Table I-C are those of this work and should be accurate to 5%. The lack of agreement with Demtröder is unexplained. Scattered exciting radiation amounting to only 10% of the fluorescent radiance in his measurements could explain the difference. Penkin and Shabanova[41] have measured relative f-values for 38 aluminum lines. They placed their values on an absolute scale using $f_{394.4} = 0.15\pm0.04$ which was determined by simultaneous dispersion and absorption measurements. In view of the uncertainties of their technique the close agreement with the work reported here is gratifying.

Table I-C. Aluminum absorption f-values

Transition	λ(nm)	Selected values (A)	(B)	(C)	(D)	This work	Recommended value
$4^2S_{1/2} - 3^2P_{1/2}$	394.4	0.122	0.15		0.075	0.11	0.11
$4^2S_{1/2} - 3^2P_{3/2}$	396.15	0.121	0.15		0.078	0.11	0.11
$3^2D_{3/2} - 3^2P_{1/2}$	308.22		0.22		0.19	0.173	0.173
$3^2D_{3/2} - 3^2P_{3/2}$	309.28					0.017	0.017
$3^2D_{5/2} - 3^2P_{3/2}$	309.27		0.23	0.158	0.20	0.157	0.157

A. Demtroder, phase-shift lifetime[20]

B. Penkin and Shabanova, hook[41]

C. Budick, level-crossing lifetime[50]

D. Corliss and Bozmann, emission[2]

3. Gallium

In contrast to aluminum, most of the work on gallium f-values has been done to obtain absolute values with little measurement of relative values alone. Allen and Assad[42] using emission from an arc with dilute copper alloy electrodes obtained $f_{403.3} = 0.049$ and $f_{417.2} = 0.054$. These values were later revised[51] to $f_{403.3} = 0.18$; and $f_{417.2} = 0.19$ but there is some confusion because of inconsistencies in the reported numbers. Ostrovskii, Penkin and Shabanova[52,53] used the hook method to obtain Nf values for the 5^2S-4^2P and 4^2D-4^2P multiplets from which they obtained absolute f-values using gallium vapor pressure data from Speiser and Johnston.[54] Their values are in Table I-D. Penkin and Shabanova[40,41,55] have extended this work to include 24 lines of the sharp and diffused series. They[56] have recently used simultaneous dispersion and absorption to determine $f_{403.3} = 0.120 \pm 0.008$ and $f_{417.2} = 0.125 \pm 0.009$.

The lifetime of the $5^2S_{1/2}$ state has been measured by Demtröder[20,49] who got 9.88 ± 0.15 nsec from which he calculated $f_{403.3} = 0.0878$ and $f_{417.2} = 0.0854$. Demtröder has indicated that his lifetime value may be too long by 6% because limited sensitivity of his apparatus made lifetime measurements impossible at gallium densities low enough to eliminate radiation entrapment.[57] Ottinger and Ziock[58] have also measured the $5^2S_{1/2}$ state lifetime using the phase-shift method and obtained 9.7 ± 2.4 nsec. Lawrence, Link and King[59] obtained absolute f-values by measuring absorption in an atomic beam. Their results are given in Table I-D. Gruzdev[48] has calculated f-values for several transitions which agree fairly well with experimental results for the sharp series but poorly for the diffused series.

Table I-D. Gallium absorption f-values

Transition	λ(nm)	Selected values (A)	(B)	(C)	(D)	(E)	This work	Recommended value
$5^2S_{1/2} - 4^2P_{1/2}$	403.30	0.129	0.0878	0.072	0.120	0.133	0.108	0.108
$5^2S_{1/2} - 4^2P_{3/2}$	417.21	0.135	0.0854	0.076	0.125	0.12	0.114	0.114
$4^2D_{3/2} - 4^2P_{1/2}$	287.42	0.318		0.23		0.365	0.271	0.27
$4^2D_{3/2} - 4^2P_{3/2}$	294.42	0.038		0.022		0.06	0.0265	0.027
$4^2D_{5/2} - 4^2P_{3/2}$	294.36	0.287		0.19		0.375	0.253	0.25

A. Ostrovskii and Penkin, hook[53]

B. Demtröder, phase-shift lifetime[20]

C. Lawrence, et al., atomic beam[59]

D. Penkin and Shabanova, hook and absorption[56]

E. Corliss and Bozmann, emission[2]

The justifications for Russell-Saunders coupling is not as strong for gallium as for aluminum. In fact, the relative f-values for the 403.3 and 417.2 nm lines from previous work indicate that it does not hold for the 5^2S-4^2P transition. The evidence for the 4^2D-4^2P transition is less convincing but there is no doubt some deviation from the Russell-Saunders case. In calculating the f-values from the lifetime measured in this work the ratio $f_{403.3}/f_{417.2}$ was taken to be 0.95. Russell-Saunders coupling was assumed for the other lines. The recommended values are those for this work and should be accurate to 5-10%. The recommended values agree with the work of Penkin and Shabanova[41,56] within their estimated uncertainty. The values of Lawrence et al.[59] appear to be too low which would indicate their estimate of the atomic beam density was too great. It is very likely that their beam contained gallium oxide which may account for this error.

4. Indium

Payne-Scott[60] used an arc to measure the relative radiances for the first sharp doublet to be $L_{410.2}/L_{451.1} = 1.62 \pm 0.09$; this corresponds to $f_{451.1}/f_{410.2} = 1.14$. Kunisz[34] obtained $f_{451.1}/f_{410.2} = 1.22$ using the same technique. Ostrovskii and Penkin and Shabanova[52,53] used the hook method together with the vapor pressure data of Anderson[61] to obtain absolute values which are given in Table I-E. They later checked these results[62] using simultaneous dispersion and absorption and obtained good agreement; $f_{410.2} = 0.20$. Penkin and Shabanova[40] extended the hook method results to include about thirty lines of the sharp and diffused series. They placed their results on an absolute scale by using Nf values of Ostrovskii and Penkin and the vapor pressure equation selected by

Table I-E. Indium absorption f-values

Transition	λ(nm)	Selected values (A)*	(B)*	(C)	(D)	(E)	(F)	This work	Recommended value
$6^2S_{1/2} - 5^2P_{1/2}$	410.2	0.201	0.144	0.120	0.172	0.105	0.24	0.118	0.12
$6^2S_{1/2} - 5^2P_{3/2}$	451.1	0.218	0.157	0.111		0.115	0.17	0.131	0.13
$5^2D_{3/2} - 5^2P_{1/2}$	303.9	.503	0.36	0.28	0.34		0.50	0.31	0.29
$5^2D_{3/2} - 5^2P_{3/2}$	325.86	.079	0.044	0.026			0.115	0.028	0.032
$5^2D_{5/2} - 5^2P_{3/2}$	325.6	.509	0.37	0.24			0.50	0.302	0.30

A. Ostrovskii et al., hook[52]

B. Penkin and Shabanova, hook[40,55]

C. Lawrence et al., atomic beam[59]

D. Moise, absorption tube[65]

E. Hulpke et al., phase-shift lifetime[67]

F. Corliss and Bosmann, emission[2]

* These results are not directly comparable since different vapor pressure data were used.

Nesmeyanov.[63] Penkin and Shabonova[55] have also revised the value for the 325.86 nm line. These revised results are shown in Table I-E. In the most recent hook method experiments Penkin and Shavanova[56] have used simultaneous measurement of total absorption and dispersion to obtain $f_{410.2}$= 0.141 ± 0.006 and $f_{451.1}$ = 0.153 ± 0.007; in good agreement with the revised values discussed above.

Ch'en and Smith[64] have obtained $f_{410.2}$ = 0.100 and $f_{451.1}$ = 0.096 using absorption techniques together with pressure broadening. Lawrence et al.[59] measured total absorption in an atomic beam and got the results shown in Table I-E. Moise[65] has used an absorption tube technique[66] to determine $f_{410.2}$ = 0.172 ± 0.0022 and $f_{303.9}$ = 0.34 ± 0.013. Hulpke, Paul and Paul[67] have measured the lifetime of the $6^2S_{1/2}$ state using the phase shift method and have obtained 8.531 ± 0.085 nsec. Based on this lifetime and relative fluorescence radiance, they calculated $f_{410.2}$ = 0.105 and $f_{451.1}$ = 0.115. Hanus[47] has calculated the ratio of f-values to be $f_{451.1}/f_{410.2}$ = 0.69 and $f_{325.6,\ 325.9}/f_{303.9}$ = 0.77. Gruzdev[48] has calculated f-values for several multiplets of the sharp and diffuse series and, as in the case of aluminum and gallium, found reasonable agreement only for the sharp series.

The f-values for the 6^2S-5^2P transition based on the lifetime reported here were calculated assuming $f_{451.1}/f_{410.2}$ = 1.09 which is the ratio obtained by the hook method and by Hulpke et al.[67] The disagreement with Lawrence et al.[59] may be due to under population of the $^2P_{3/2}$ level in the atomic beam, as they have mentioned. It is interesting that this ratio agrees more closely with that expected for Russell-Saunders coupling than in the corresponding transition for gallium. The f-values for the 5^2D-5^2P transition were calculated assuming Russell-Saunders coupling. The recommended f-values for the

6^2S-5^2P transition are those from this work. The f-values for the 5^2D-5^2P transition are selected to preserve the relative values obtained by the hook method but normalized to the lifetime measured here.

5. Thallium

A great deal of work has been done on thallium, must of it prior to 1950.[32] Most of this work has been carefully reviewed and evaluated by Gallagher and Lurio[4] and will not be discussed in detail here. They have given f-values for 25 thallium lines which they have placed on an absolute scale using their value of the lifetime of the $^2S_{1/2}$ state, 7.5±0.3 nsec, which is an average of optical double resonance and level crossing results. The ratio $A(7^2S_{1/2}-6^2P_{3/2})/A(7^2S_{1/2}-6^2P_{1/2})$ = 1.13±0.05 which they used is an average of their results and that of Kvater.[68] Gallagher and Lurio[4] also used level crossings to determine the lifetime of the $6^2D_{3/2}$ state to be 6.2±1.0 nsec.

Gough and Series[69] have also used the level crossing technique to measure $\tau(6^2D_{3/2})$ = 5.2±0.8 nsec. Lawrence et al.[59] used absorption by an atomic beam to determine the f-values shown in Table I-F. Gruzdev[48] and Anderson et al.[70] have calculated f-values for thallium which show fair agreement with experimental values.

The f-values for the 377.6 and 535.0 nm lines obtained in this work were calculated from the lifetime of the $7^2S_{1/2}$ state using the ratio of transition probabilities $A(7^2S_{1/2}-6^2P_{3/2})/A(7^2S_{1/2}-6^2P_{1/2})$ = 1.105 which Gallagher and Lurio[4] obtained from the data of Kvater.[68] The f-values for the 276.8 and 352.9 nm lines were calculated from the lifetime of the $6^2D_{3/2}$ state assuming the ratio $f_{276.8}/f_{352.9}$ = 7.05 of Penkin and Shabanova.[55]

Table I-F. Thallium absorption f-values

Transition	λ(nm)	Selected values (A)	(B)	(C)	This work	Recommended value
$7^2S_{1/2}$-$6^2P_{1/2}$	377.57	0.133	0.127	0.11	0.133	0.133
$7^2S_{1/2}$-$6^2P_{3/2}$	535.05	0.151		0.23	0.147	0.147
$6^2D_{3/2}$-$6^2P_{1/2}$	276.79	0.290	0.30	0.24	.292	0.308
$6^2D_{3/2}$-$6^2P_{3/2}$	352.94	0.040		0.28	..034	0.038
$6^2D_{5/2}$-$6^2P_{3/2}$	351.92	0.346		1.1		0.329

(A) Gallagher and Lurio, level crossing lifetime[4]

(B) Lawrence et al., atomic beam[59]

(C) Corliss and Bozmann, emission[2]

The recommended f-values for thallium are those obtained in this work for 377.6 on 535.0 nm. The value of $f_{276.8}$ is based on the ratio $f_{377.6}/f_{276.8} = 0.427$ from Penkin and Shabanova.[55] Gallagher and Lurio used 0.461 for this ratio which is the value of Prokof'ev and Filippov,[71] but Penkin[72] has indicated that this value is probably the less reliable of the two because of systematic errors introduced by use of a prism spectrograph. The f-values for 352.9 and 351.9 nm are calculated from the relative measurements of Penkin and Shabanova. The $6^2D_{3/2}$ state lifetime calculated from the recommended f-values if 6.5 nsec. which is somewhat lower than that obtained here but agrees within estimated uncertainties. The good agreement with the atomic beam absorption results[59] is encouraging.

6. Copper

In 1936, Van Lingen[73] reported relative transition probabilities for 10 copper lines, including the five transitions which depopulate the 4^2P^o state. Later Schuttevaer et al.[74] indicated that some of Van Lengen's values were in error because of inaccurate temperature estimates of his arc, but this should not effect the relative values of lines depopulating the 4^2P^o state since the splitting of that state is small. Allen and Assad[42] use arc emission to determine absolute f-values for a large number of copper lines but indicated their results were probably inaccurate, particularly in the case of the main resonance lines. Addink[43] measured $f_{324.7} = 0.13$ using arc emission. Riemann[29] has also used arc emission to obtain absolute f-values for a number of copper lines. His values are given in Table I-G. Dickerman and Deuel[75] have measured relative transition probabilities for 12 copper lines in the 400-510 nm region but not including the resonance lines.

King and Stockbarger[76] measured absorption by a column of copper vapor heated in a tube furnace to determine the f-values for the resonance lines; $f_{327.4} = 0.32 \pm 0.03$ and $f_{324.7} = 0.62 \pm 0.06$. Davis, Routley and King[77] redetermined these values using absorption from an atomic beam and obtained $f_{327.4} = 0.21$ and $f_{324.7} = 0.32$. This work was continued by Bell et al.[78] and the most recent atomic beam results are $f_{327.4} = 0.16 \pm 0.04$ and $f_{324.7} = 0.31 \pm 0.03$. The work of King and Stockbarger[76] has been re-evaluated by Bell et al.[78] in view of more reliable vapor pressure data and the original f-values reduced by about 30%. Ostroumenko and Rossikhin[79] have measured the relative f-values of the main resonance lines and found $f_{324.7}/f_{327.4} = 1.927$. The most recent absorption measurements are those of Moise[80] who has used a step-cell absorption technique[65,66] to determine $f_{327.4} = 0.153$ and $f_{324.7} = 0.322$.

The hook method was used by Parchevskii and Penkin[36] to determine $f_{324.7}/f_{327.4} = 1.98$. Ostrovskii and Penkin[30] have used the hook method to determine absolute values for these transitions as well as the ratio $f_{324.7}/f_{510.6} = 68$. Slavenas[81] revised the values of Ostrovskii and Penkin using the more reliable vapor pressure data of Nesmeyanov[63] and obtained $f_{327.4} = 0.323 \pm 0.004$ and $f_{324.7} = 0.66$ as well as f-values for 7 other lines in the ultraviolet. Bucka, Ney and Hepple[82,83] and Levin and Budick[84] have used the level-crossing technique to obtain 7.0 ± 0.2 nsec and 7.2 ± 0.7 nsec respectively for the lifetime of the $4^2P^o_{3/2}$ state.

Only a few theoretical calculations have been made for transition probabilities of copper. Varsovsky[85] has used a charge-expansion method and obtained results which agree well with the original experimental results of Kind and Stockbarger.[76] Stewart and Rotenberg[86] have used semi-empirical wave functions to calculate $f_{324.7} = 0.62$. Bialas-Zabawa et al.[87] have

calculated the ratio $f_{324.7}/f_{327.4} = 1.996$.

It is difficult to infer f-values from the copper lifetime measured here since it was not possible to separate the $4^2P^o_{1/2}$ and $4^2P^o_{3/2}$ levels. There is also the probability of decay to the 4^2D state. In calculating the f-values therefore, it was assumed that the lifetimes of the $4^2P^o_{1/2}$ and $4^2P^o_{3/2}$ levels are equal and that the branching ratio from each of these levels to the $4^2S_{1/2}$ state is 0.985. This value is based on the measurement of Riemann.[29] Russell-Saunders coupling was assumed for the 4^2P^o-4^2D transition.

Comparison of the values thus calculated with those of previous work seem to indicate that the assumption of equal lifetimes for the $^2P^o$ levels is not correct. If the lifetime of the $^2P^o_{3/2}$ state is taken to be 7.1 nsec, which is the average of the level-crossing results[82-84] and the ratio $f_{324.7}/f_{327.4} = 2.07$, the average for the values in Table I-G, the lifetime of the $^2P^o_{1/2}$ state is calculated to be 7.46 nsec. The branching ratio to the $^2S_{1/2}$ state is still assumed to be 0.985. The weighted average of these lifetimes, which corresponds to what has been measured in this work, would be given by $(2/3\ \tau\ ^2P^o_{3/2} + 1/3\ \tau\ ^2P^o_{1/2})$. This gives 7.22 nsec which is in good agreement with the 7.2±0.3 nsec measured here. The f-values calculated on this basis are those recommended for the $4^2P^o_{1/2}$-$4^2S_{1/2}$ transition. The f-values for the 4^2P^o-4^2D transition are calculated from the above lifetimes assuming a branching ratio of 0.015 and Russell-Saunders coupling.

7. Silver

The earliest reported study of silver was done by Filippov and Islamov[88,89] who used the hook method to obtain the ratio $f_{328.1}/f_{338.3} = 2.03\pm0.06$. More recent application of the hook method by Penkin and

Table I-G. Copper absorption f-values

Transition	λ(nm)	Selected values (A)	(B)	(C)	(D)	(E)	(F)	This work	Recommended value
$4^2P^o_{1/2}$ - $4^2S_{1/2}$	327.40	2276.0	0.14	0.16	0.153	.323	0.155	0.220	0.212
$4^2P^o_{3/2}$ - $4^2S_{1/2}$	324.76	4790.0	0.287	0.31	0.322	.66	0.32	0.433	0.439
$4^2P^o_{1/2}$ - $4^2D_{3/2}$	578.21	5.2	0.00337				0.0068	0.0052	0.00504
$4^2P^o_{3/2}$ - $4^2D_{3/2}$	570.02	1.00	.004				0.0017	0.00075	0.00076
$4^2P^o_{3/2}$ - $4^2D_{5/2}$	510.55	10.0	.0033				0.0033	0.0051	0.0051

A. Van Lingen, emission, relative[73]

B. Reimann, emission[29]

C. Bell et al., atomic beam[78]

D. Moise, absorption tube[80]

E. Slavenas, hook[81]

F. Corliss and Bozmann, emission[2]

Slavenas,[90] using the vapor pressure data of Nesmeyanov,[63] gives $f_{338.3} = 0.247 \pm 0.004$ and $f_{328.1} = 0.506 \pm 0.004$. Allen and Asaad[42] using emission from an arc with copper alloy electrodes obtained $f_{338.3} = 0.14$. This value was later revised by Allen[51] but the new value is not clear. Hinnov and Kohn[91] obtained $f_{338.3} = 0.22$ and $f_{328.1} = 0.39$ using emission from an acetylene-air flame. Addink[43] using arc emission obtained $f_{328.1} = 0.1$.

The absorption tube method has been used by Bieniewsky[92] to obtain $f_{338.3} = 0.28 \pm 0.03$ and $f_{328.1} = 0.52 \pm 0.05$. Lawrence, Link and King[59] measured absorption by an atomic beam and obtained $f_{338.3} = 0.215 \pm 0.02$ and $f_{328.1} = 0.45 \pm 0.05$. The most recent absorption results are those of Moise[65,80] who used a stepped absorption cell and got $f_{338.3} = 0.196 \pm 0.015$ and $f_{328.1} = 0.459 \pm 0.034$. Levin and Budick[84] have used the level-crossing method to measure the lifetime of $^2P^o_{3/2}$ state and got 7.4 ± 0.7 sec. The lifetime of the $^2P^o_{3/2}$ state has also been measured by Bucka, Ney and Heppke,[82] again from level-crossings, and they got 6.7 nsec. Bialas-Zabawa et al.[87] have calculated the ratio $f_{328.1}/f_{338.3} = 1.98$.

The determination of f-values from the lifetimes measured here is straight-forward for silver since each level depopulates by only one transition. The values obtained, $f_{338.3} = 0.229 \pm 0.012$ and $f_{328.1} = 0.482 \pm 0.030$ have been taken as the recommended values primarily because of the good agreement with level crossing results[82] and relative values of the hook method.[90]

Table I-H. Silver absorption f-values

Transition	λ(nm)	Selected values (A)	(B)	(C)	(D)	(E)	(F)	This work	Recommended value
$5^2P^o_{1/2} - 5^2S_{1/2}$	338.29	0.247	0.215	0.196			0.12	0.23	0.23
$5^2P^o_{3/2} - 5^2S_{1/2}$	328.07	0.506	0.45	0.459	0.48	0.44	0.27	0.48	0.48

A. Penkin and Slavenas, hook[90]

B. Lawrence et al., atomic beam[59]

C. Moise, absorption tube[80]

D. Bucka et al., level crossing lifetime[82]

E. Levin and Budick, level crossing lifetime[84]

F. Corliss and Bozmann, emission[2]

8. Sodium

A very great amount of work has been done on the determination of f-values for the sodium D lines. The measurement of the sodium lifetime in this work was done as a check for possible systematic errors in the phase-shift method, since the lifetime is considered to be well established. A value of $\tau 3^2P = 16.1 \pm 0.2$ nsec would embrace nearly all of the measurements made in the last decade and is in good agreement with much of the very early work.[1] Table I-I gives a summary of the more recent measurements of the 3^2P state lifetime. The only value falling significantly outside the limits of the recommended value is that of Karstensen and Schramm.[93] They used the phase-shift technique with electron excitation and may have had serious systematic errors.

The ratio $f_{589.0}/f_{589.6}$ is certainly very close to 2.0. Ostrovskii and Penkin[94] using the hook method got 1.98 ± 0.01. The absorption f-values for sodium can be taken as $f_{589.0} = 0.650$ and $f_{589.6} = 0.328$. These values are certainly correct to within 2%.

9. Cesium

The lifetime of the $7^2P_{3/2}$ state of cesium was measured primarily to check results obtained by Wolff[6,100] so as to provide a basis for comparison of iodine lifetimes measured in the two laboratories,[8,101] (Part II of this thesis). The value obtained here, $\tau 7^2P_{3/2} = 114 \pm 4$ nsec, is in good agreement with the 111 ± 6 nsec obtained by Wolff.

The determination of f-values from the measured lifetime of the $7^2P_{3/2}$ state is particularly difficult because this state can radiate to the 7^2S and 5^2D states with relatively large probability. Radiation to these states lies far to the red (see Fig. I-9) and no experimental

Table I-I. Lifetime of the 3^2P state of sodium

Lifetime (nsec)	Method of Measurement	Reference
15.9±0.016	Phase-shift	49,20
15.6±0.8*	Hook	94,95
15.95±0.4	Magnetic depolarization	96
15.9±0.039	Phase-shift	67
16.3±0.5	Level crossing	97
14.2±0.2	Phase-shift, electron excitation	93,98
16.1±0.7	Optical double resonance	99
16.1±0.3	Phase-shift	16
16.3±0.4	Direct decay	25
16.1±1.0	Direct decay	6,100

* Calculated from relative f-values assuming f-sum = 1.0±0.05.[95]

work has been done on these transitions. This has led to some confusion in interpreting previous results as Link[102] has pointed out.

Calculations in three papers[103-105] have included all the transitions of interest. Their results are shown in Table I-J. Agreement among calculated f-values is good except for the 7^2P-5^2D f-values of Stone[104] which appear to be about two orders of magnitude too large. The good agreement between the lifetimes calculated by Heavens,[103] using the Coulomb approximation method of Bates and Damgaard,[45] and experimental results for alkali metal lifetimes, is indicated in Table I-K. A problem with the Coulomb approximation calculation is that it gives 2.7 for the ratio $f_{455.5}/f_{459.3}$ while the hook method experimental value for this ratio is 4.3.[106,107] The experimental results of Kvater and Meister,[106] who used the hook method, and of Minkowski and Muhlenbruch,[108] who used magneto-rotation, are shown in Table I-J. Both of these experimental results reflect the uncertainty in cesium vapor pressure. No attempt has been made to select recommended f-values for cesium.

10. Mercury

The lifetime of the $^3P_1^o$ state of mercury is well known and was measured here as a check for systematic errors in the 1 MHz ultrasonic modulating system. A value of $\tau\,^3P_1^o = 116 \pm 2$ nsec, corresponding to $f_{2537} = 0.0254 \pm 0.0005$ would bracket all of the recent determinations within their uncertainties. Early work has been reviewed by Mitchell and Zemansky.[1] A long series of measurements using the double resonance technique has been conducted by a group in France. Their latest results[113] give $\tau = 116$ nsec. Schuler[114] has examined the effect of microwave power on the double resonance results and obtained $\tau = 114$ nsec.

Table I-J. Cesium absorption f-values

Transition	λ(nm)	Selected values (A)	(B)	(C)	(D)	(E)	(F)
$7^2P_{1/2}$-$6^2S_{1/2}$	459.32	0.0042	0.0067	0.0028	0.003	0.0027	0.11
$7^2P_{3/2}$-$6^2S_{1/2}$	455.54	0.0160	0.0184	0.0174	0.013	0.012	0.21
$7^2P_{1/2}$-$7^2S_{1/2}$	3095.0	1.58	0.505	0.556			
$7^2P_{3/2}$-$7^2S_{1/2}$	2931.8		1.044	1.115			
$7^2P_{1/2}$-$5^2D_{3/2}$	1375.7		0.023	0.652			
$7^2P_{3/2}$-$5^2D_{5/2}$	1342.7	0.24	0.0035	0.208			
$7^2P_{3/2}$-$5^2D_{5/2}$	1360.5		0.020	1.533			

A. Anderson et al., calculation[70,105]

B. Heavens, calculation[103]

C. Stone, calculation[104]

D. Kvater and Meister, hook[106]

E. Minkowski and Muhlenbruch, magneto-rotation[108]

F. Corliss and Bozmann, emission[2]

Table I-K. Comparison of experimental and calculated lifetimes for alkali metals

Elements	Excited state	Lifetime (nsec)	
		Calculated[a]	Measured
Na	3^2P	17.0	See Table I-I
	4^2D	53.5	52.1±0.3[b]
K	$4^2P_{3/2}$	27.0	27.8±0.5[c] 26.0±0.5[d]
	$5^2P_{3/2}$	121.0	140.8±1.0[d]
Rb	$5^2P_{3/2}$	26.7	27.0±0.5[c] 27.8±0.9[e]
Cs	$6^2P_{3/2}$	30.9	30.5±0.6[c]
	$7^2P_{3/2}$	121.0	114.0±4.0[f] 118[g] 111.0±6.0[h]
	$8^2P_{3/2}$	267.0	240 ±20.0[i]

a - Heavans, Coulomb approximation[103]

b - Karstensen and Schramm, phase shift[93]

c - Link, phase-shift[16]

d - Schmieder et al., level-crossing[109]

e - Stephenson, magneto-rotation[110]

f - This work

g - Bucka et al., level-crossing[111]

h - Wolff, direct decay[6,100]

i - Bucka and Oppen, level-crossing[112]

Lurio[115] cites unpublished results of Kaul, who used level crossings to get τ = 115 nsec. Recent photon correlation results of Nussbaum and Pipkin[116] give 114±14 nsec. Chutjian[8] used the phase-shift technique to get 110±5 nsec. The 115±3 obtained in this work agrees well with these prior results and indicates that systematic errors in the 1 MHz system are small.

11. Lead

A large number of lead lines lie in the visible spectrum and are of considerable astrophysical interest. Only those lines which depopulate the $7s^2P_1^o$ level will be considered (see Fig. I-9). The branching ratio for the $7^2P_1^o - 6^1S_0$ (1718.0 nm) transition is expected to be very small and will be neglected.

The f-value for the 283.3 nm line was first measured by Engler[117] who observed absorption by an atomic beam to determine $f_{283.3} = 0.60\pm0.06$. Allen and Asaad[42,51] used emission from an arc with copper alloys electrodes to obtain $f_{364.0} = 0.25$ and $f_{405.8} = 0.35$. Bell and King[118] used their atomic beam absorption technique to measure $f_{283.3} = 0.23\pm0.02$. Khokhlov has conducted a number of absorption and emission experiments on lead lines. His most recent work[119] obtained relative f-values for the lines of interest here from relative radiance of a hollow cathode discharge lamp. These results are shown in Table I-L. Penkin and Slavenas[120] have also obtained relative f-values by the hook method, as shown in Table I-L, as well as $f_{283.3} = 0.212$.

Lvov[121] has used flash heating of a known quantity of material to produce a vapor of known density. By measuring absorption by the vapor he obtained $f_{283.3} = 0.077\pm0.015$. Brown[122] has observed emission from

Table I-L. Lead absorption f-values

Transition	λ(nm)	Selected values (A)	(B)	(C)	(D)	(E)	This work	Recommended value *
$7^3P_1^o$-6^3P_0	283.31	100.0	100.0	0.21		0.22	0.161	0.168
$7^3P_1^o$-6^3P_1	363.95	46.7	29.7	0.17	0.039	0.86	0.045	0.047
$7^3P_1^o$-6^3P_2	405.78	142.0	72.0	0.365	0.139	0.41	0.136	0.142
$7^3P_1^o$-6^1D_2	722.90	31.0				0.011	0.064	0.067

A. Khohklov, emission rel.[119]

B. Penkin and Slavenas, hook rel.[120]

C. Helliwell, calculation[124]

D. Brown, emission[122]

E. Corliss and Bozmann, emission[2]

*. See text for other data considered

shock heated lead and determined $f_{364.0} = 0.039 \pm 0.012$ and $f_{405.8} = 0.139 \pm 0.04$. Salomon and Happer[31] have reported an extensive level-crossing study on the $7^3P_1^o$ level of lead. They determined the lifetime of that state to be 5.75 ± 0.2 nsec and, from the observed coherence-narrowing effects, determined the branching ratio of the $7^3P_1^o - 6^3P_0$ (283.3 nm) transition to be 0.27 ± 0.03. They also used early work by Khokhlow to determine f-values for the 364.0 and 405.8 nm lines. deZafra and Marshall[123] have also used level crossings to obtain $\tau = 5.6 \pm 0.7$ nsec and using relative values from the hook method conclude $f_{283.3} = 0.197 \pm 0.03$. Helliwell[124] has calculated f-values as shown in Table I-L.

In determining f-values based on the lifetime measured here, the bramching ratio for the 283.3 nm line was taken as 0.27 and the relative f-values of Khokhlov[119] used to determine the other lines. The use of Khokhlov's relative values is somewhat arbitrary. His relative f-value for the 283.3 nm line seems too small compared to the other lines but this is probably due to absorption in the source since the line connects with the ground state. The ratio $f_{405.8}/f_{384.0}$ is 3.6, 2.4, and 3.0 for Brown, Penkin, and Khokhlov, respectively and Khokhlov's value is intermediate. The recommended values followed this same procedure but took the lifetime as 5.8 nsec, an average of the lifetime results.

12. Bismuth

Relatively little work has been done on bismuth f-values. Only three papers have considered lines originating from the $^4P_{1/2}$ level. Corliss and Bozmann[2] give $f_{306.8} = 0.25$ and $f_{477.2} = 0.015$ but their measurements did not extend to the 915.0 nm line. Their values indicate a branching ratio of 0.026 for the $^4P_{1/2} - ^2D_{3/2}$ transition. No value

for the branching ratio for $^4P_{1/2}$-$^2P_{3/2}$ is available but it is surely less than 0.01. Rice and Ragone[125] employed an absorption method designed to determine both the f-value of a line and the vapor pressure. They obtained $f_{306.8} = 0.131^{+0.061}_{-0.039}$. Lvov[121] used absorption to obtain $f_{306.8} = 0.077 \pm 0.015$. The f-value calculated from this work, assuming a branching ratio of 0.97 for the $^4P_{1/2}$-$^4S^o_{3/2}$, is 0.116 ± 0.005 and is the recommended value.

13. General

Comparison of the results obtained here with other phase-shift lifetimes shows generally poor agreement, except in the case of Na 3^2P. It seems probable that these differences arise from the effects of scattered exciting radiation and radiation entrapment in the previous work. More striking is the very good agreement between this work and the results of level crossing measurements. In most cases (Al $3^2D_{3/2}$, Tl $7^2S_{1/2}$, Cu $4^2P^o_{3/2}$, Na $3^2P^o_{3/2}$, Hg $6^3P^o_1$, and Pb $7^3P^o_1$) agreement is better than 5%. The only case where agreement is poorer than 10% is that of Tl $6^2D_{3/2}$ for which the level crossing technique does not give unambiguous results. In this case the high-field level crossings cannot be resolved[4,69] and the lifetime must be determined from the zero field crossings (Hanke-effect). In order to enterpret the experimental results, the relative populations of the hyperfine levels must be known, which implies that the detailed nature of the exciting radiation be known. In practice the degree of self reversal of the two hyperfine components is not known accurately and this uncertainty must be reflected in the lifetime measurement. Absorption results vary considerably and there seems to be no a priori way of determining when they will be reliable.

This is also true for emission measurements where, in addition, it seems particularly difficult to evaluate absorption within the source.

Comparison with hook method results shows general agreement within the uncertainties in vapor pressure. In three cases (Ag, In, Cu) the hook method results were recalculated using the best available vapor pressure data.[21] For silver, where the hook method f-values are about 6% greater than the recommended value, and for copper, where the hook method f-value is about 50% greater than the recommended value, there was no significant change in the corrected hook method results. For indium, use of the best vapor pressure data increased the difference between the hook method f-value and the recommended value from 20% to 100%. These results indicate that there are other uncertainties than vapor pressure in hook method absolute f-values.

II. LIFETIMES OF SOME v' REGIONS OF THE $B^3\Pi_{0^+u}$ STATE OF I_2

A. Introduction

The lifetime of the $B^3\Pi_{0^+u}$ state of iodine has been the object of considerable attention in this laboratory,[8,13,14,27,101] the latest work being that of Chutjian. He found that the lifetime of the B state varied widely as a function of the vibrational region studied. Within the approximation of separability of the electronic, vibrational and rotational energies, the lifetime of a particular v' level is given by

$$(\tau_{v'})^{-1} = \sum_{v''} A_{v'v''} = \frac{64\pi^4}{3h} |R_e|^2 \sum_{v''} \lambda^{-3} q_{v'v''} \qquad \text{(II-1)}$$

where $q_{v'v''}$ is the Franck-Condon factor, λ is the wavelength of the transition, R_e is the electronic part of the transition moment, (assumed to be a constant in this equation), and h is Planck's constant. The lifetimes measured by Chutjian showed variation with changing v' not consistent with the expected smooth variation of the sum on the right in Eq. (II-1).[126] The variation in lifetime could possibly be explained through spontaneous predissociation of the excited iodine molecule at a rate comparable to that for radiative decay but different for different v'. This idea has been previously discussed in detail.[8,101]

Recent measurements by Wolff,[6] using a technique which observes directly the decay of the excited state, have indicated that some of Chutjian's results are in error and that the lifetime variation with v' is more nearly that expected from Eq. (II-1); though still not smooth. It was decided to investigate the lifetime of the B state in the v' regions where there was the largest discrepancy between the work of Chutjian and Wolff using the newly developed 1.0 MHz capability of the ultrasonic

modulator. Part of Chutjian's work was also repeated using the 361 kHz wheel modulation apparatus which he used.

Excited iodine molecules can disappear upon collision with foreign gases or other iodine molecules (collisional quenching), presumably through a collision induced predissociation. This means that the measured lifetime for the excited state, in a system where no foreign gas is present, is determined by the sum of the radiative decay rate and the collisional quenching rate (plus the dissociative rate, k_d, if that is present). The radiative decay rate is just $\Sigma_{v''} A_{v'v''}$ as discussed above. The collisional quenching rate can be treated in terms of the collision frequency for a uniform gas having a collision cross section σ^2 (the square of the collision diameter). For iodine at room temperature (300 K) the quenching rate is[8] $(2.264\times10^3)\ \sigma^2 P$ where P is the iodine pressure in Torr, and σ^2 is in nm^2. Consequently the measured lifetime τ is given by

$$\frac{1}{\tau} = \sum_{v''} A_{v'v''} + (2.264\times10^3)\ \sigma^2 P \qquad \text{(II-2)}$$

In a plot of $1/\tau$ vs P, the radiative lifetime, $\tau_{v'}$, can be obtained from the intercept and σ^2 from the slope. If spontaneous predissociation takes place the plot will give a lifetime shorter than $\tau_{v'}$.

B. Apparatus and Procedures

The lifetime measurements made at 1.0 MHz modulation used the ultrasonic modulator and associated equipment described in Part I. The lifetime measurements made at 361 kHz modulation used the rotating grating (wheel) modulator described by Chutjian[8] except for a few minor alterations outlined below. In both cases the method of measurement was the same. The modulation frequency was beat to 1.0 kHz and all amplification,

phase shifting, and phase detection is carried out at this frequency.

The wheel modulator was modified so that the wheel rotated in the vertical plane with the motor and spindle horizontal. This is the configuration for which the spindle was originally designed and provides for proper lubrication of the bearings. There have been no difficulties getting the wheel to stay "in lock."[8] The connections to the limiter and quadrature grids of the phase discriminator tube in the frequency to voltage converter (see Appendix) were reversed so that the wheel now locks in at 361 kHz instead of 359 kHz. Frequency stability was improved by this modification. The wire grating (Fig. 16 of Ref. 8) was rebuilt so as to be more uniform over a greater area. This permitted a larger area on the wheel to be illuminated. Modulated light reflected from the wheel could then be imaged on an aperture stop which in turn was imaged into the cell. This procedure had the advantage over direct imaging of reflected light into the cell, in that DC scattered light was reduced and the region of modulated light with the greatest phase homogeneity could be selected for sample excitation.

Two sample cells were used, one of which was the same cell used by Chutjian and Wolff and the other freshly filled. No measurable difference in lifetime was noted. The iodine pressure in the cell was controlled by the temperature of a side arm which extended into a closed water-filled Dewar. The water temperature was controlled by a small heater and measured with a calibrated mercury thermometer to the nearest 0.1 degree. The vapor pressure data of Shirley and Giauque were used.[127]

The light sources used are listed in Table II-A together with the wavelength isolation filters and blocking filters for excitation to the

Table II-A. Summary of experimental parameters for iodine lifetime measurements

Wavelength (nm)	Approx. v'	Source	Isolation[a] filter	Blocking filter	Photomultiplier
589.5 (Na D lines)	15	Na Osram[b]	interference filter (5.8)	Corning 2-60	RCA 7265
589.5 (filtered continuum)	15	Tungsten[c] strip lamp	interference filter (5.8)	Corning 2-60	RCA 7265
546.1 (Hg line)	25	G.E. AH4	interference filter (5.8)	Corning 2-73	RCA 7264
546.1 (filtered continuum)	25	tungsten[c] strip lamp	interference filter (5.0)	Corning 2-73	RCA 7264
508.6 (Cd line)	50	Cd Osram[b]	interference filter (2.9) Corning 4-96	Corning 3-68	RCA 7264
508.7 (filtered continuum)	50	Tungsten[c] strip lamp	interference filter Corning 4-96	Corning 3-68	RCA 7264

a - Number in parentheses after interference filter is full width at half maximum in nm.

b - Excited by square wave generator, see text.

c - G.E. Microscope illuminator 18A/T10/1P-6V, SRF filament.

different v' regions. It was noted that the interference filters, which are the same ones used by Chutjian and Wolff, have secondary transmission maxima in the red. For this reason the Corning filter listed was also used in wavelength selection at 508.7 nm.

The blocking filters used are different from those used by Chutjian. It was found that the Wratten filters which he used did not completely block the exciting radiation while the Corning filters used here did. Both types of filters fluoresce to the red of the exciting light, but the Corning filters to a lesser extent. The scattered light corrections made by Chutjian were not necessary here since the L_f/L_n ratio was always greater than 100.

During the course of the experiments it was found that the measured lifetimes, particularly in the v' = 25 region, were different for the two modulation frequencies. Since the higher frequency modulation results in rather large phase-shifts for the longer lifetimes, this difference was originally attributed to non-linear behavior of the calibrated phase-shifters. Speed of light measurements permit calibration of these phase-shifters over only the first 35°. Calibrated delay lines covering the range from 25 nsec to 550 nsec, in steps of 25 nsec, were therefore used to extend the calibration. These delays permit calibration of the 1.0 MHz system over the full 90° range of the shifter and calibration of the 361 kHz system up to 71°. The results of this calibration are shown in Fig. II-1. It can be seen that both systems measure slightly high for large shifts and that this divergence is different at the two frequencies. It could not be determined if the difference in measurement at the two frequencies was due to delay line effects or if it represents systematic error. If there is a systematic error, the actual lifetime

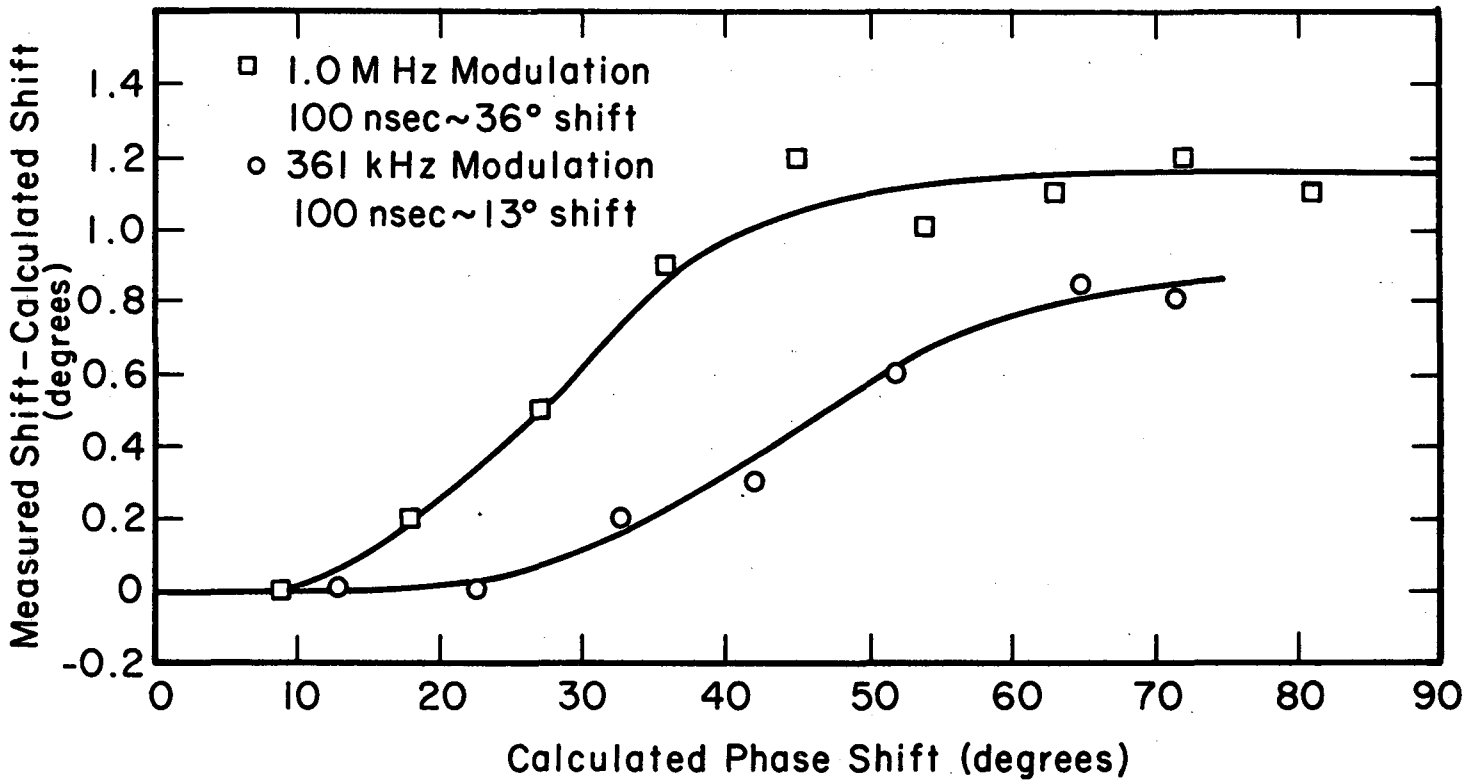

XBL 6810-6015

Fig. II-1

is shorter than the measured value. The maximum error would be about 5% for 1.0 MHz modulation and about 2% for 361 kHz modulation.

C. Results and Discussion

The measured lifetimes and collision quenching cross-sections are given in Table II-B along with the results of Chutjian[8] and Wolff.[6] Figures II-2 through II-5 show typical plots of $1/\tau$ vs iodine pressure from which the results were obtained. The errors indicated are much larger than the probable errors obtained from least squares analysis of the data which did not exceed 4%. The increased uncertainty reflects the possible systematic errors which may exist for large (greater than 30°) phase shifts. The v' range excited by the atomic line sources have been taken from Chutjian.[8] The v' range regions excited when a filtered continuum source was used have been calculated taking into account the transmission profile of the filter, the partition function of the ground state and the Frank-Condon factors.

The lifetimes measured here, while significantly different from Chutjian's results in the v' = 50 region, do not alter the basic observation that the variation in lifetime cannot be explained by the $\sum_{v''} \lambda^{-3} q_{v'v''}$ term in Eq. (II-1). The reason for the disagreement with Chutjian's work is not known but may lie in the scattered light correction which he made. He assumed that the scattered light phase was the same as that of the exciting light but did not check this experimentally. There is also the new observation that the measured lifetime of the v' ~ 25 region is a function of modulation frequency while the measured lifetimes of the v' ~ 15 and v' ~ 50 regions are not. This last observation can only result if there are at least two states emitting in the

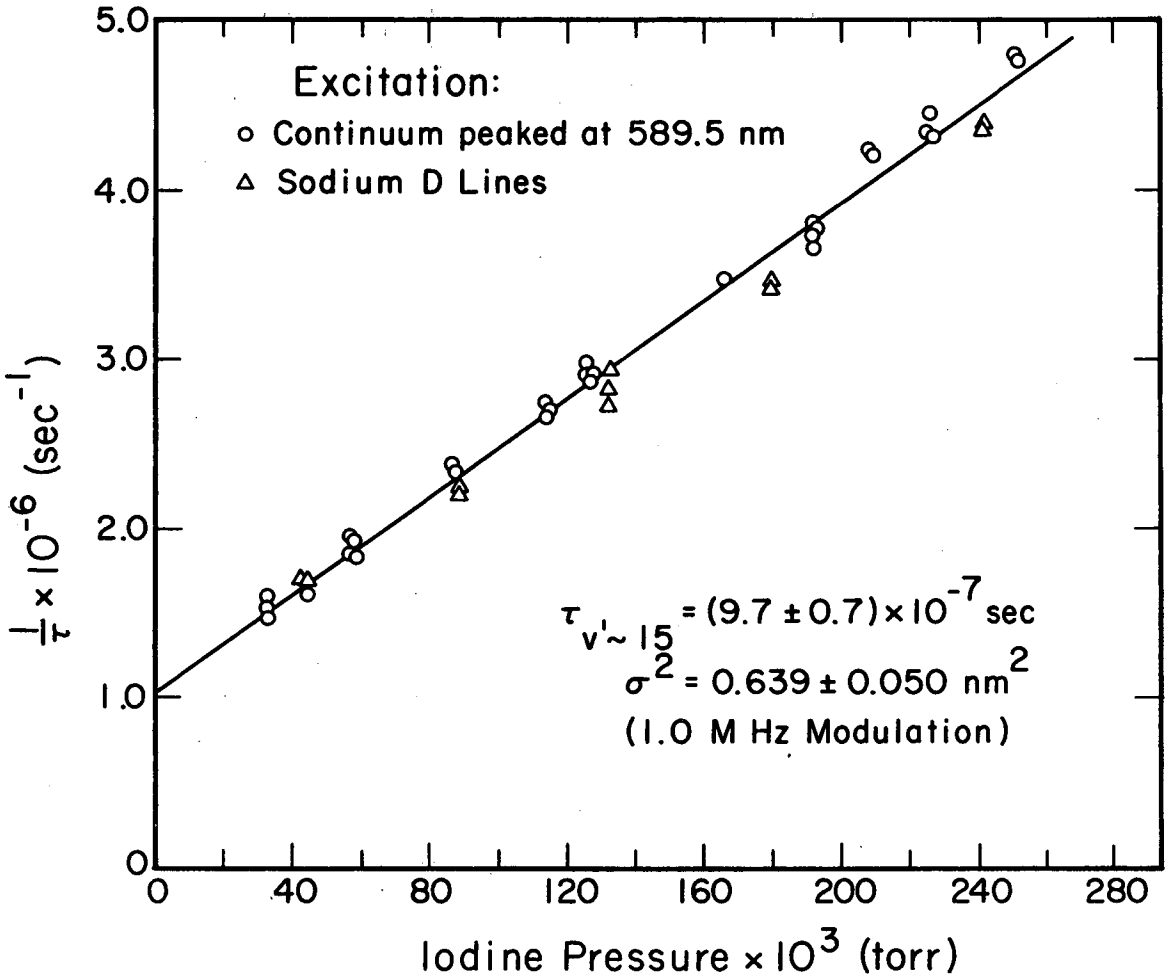
Excitation:
o Continuum peaked at 589.5 nm
Δ Sodium D Lines
$\tau_{v'\sim 15} = (9.7 \pm 0.7) \times 10^{-7}$ sec
$\sigma^2 = 0.639 \pm 0.050$ nm^2
(1.0 M Hz Modulation)
$\frac{1}{\tau} \times 10^{-6}$ (sec^{-1})
Iodine Pressure $\times 10^3$ (torr)
5.0
4.0
3.0
2.0
1.0
0
0
40
80
120
160
200
240
280
XBL 6810-6016

Fig. II-2

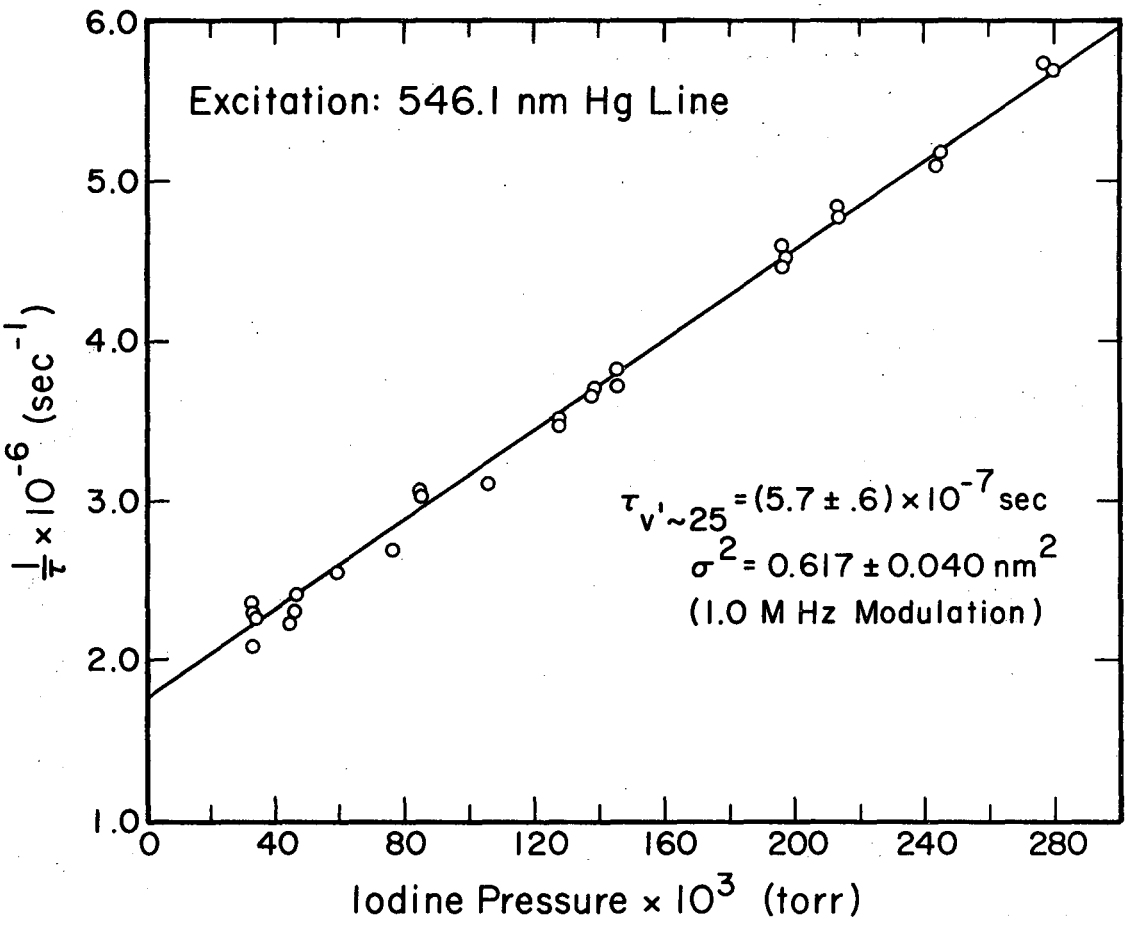

XBL 6810-6018

Fig. II-3

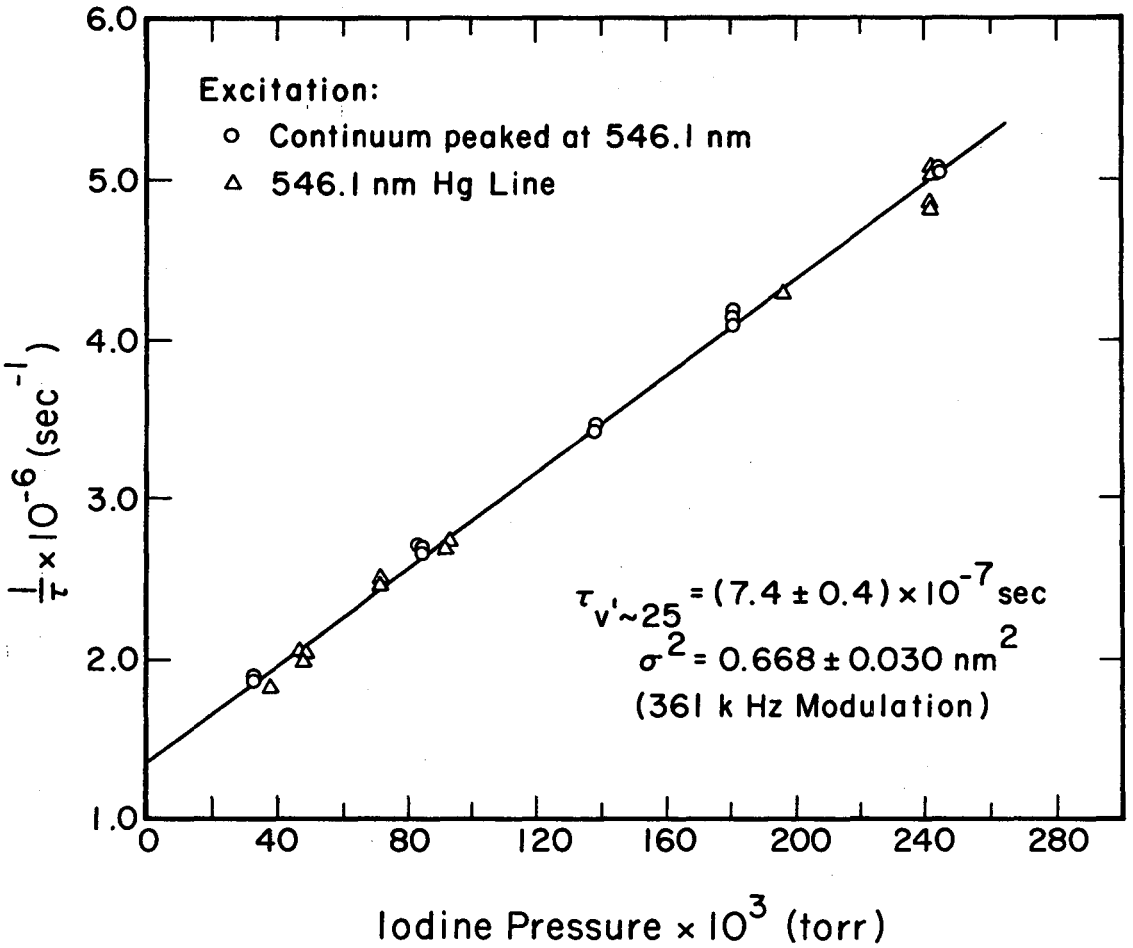
Excitation:
o Continuum peaked at 546.1 nm
Δ 546.1 nm Hg Line
$\tau_{v'\sim25} = (7.4 \pm 0.4) \times 10^{-7}$ sec
$\sigma^2 = 0.668 \pm 0.030$ nm^2
(361 k Hz Modulation)
$\frac{1}{\tau} \times 10^{-6}$ (sec^{-1})
Iodine Pressure $\times 10^3$ (torr)
6.0
5.0
4.0
3.0
2.0
1.0
0
40
80
120
160
200
240
280
XBL 6810-6017

Fig. II-4

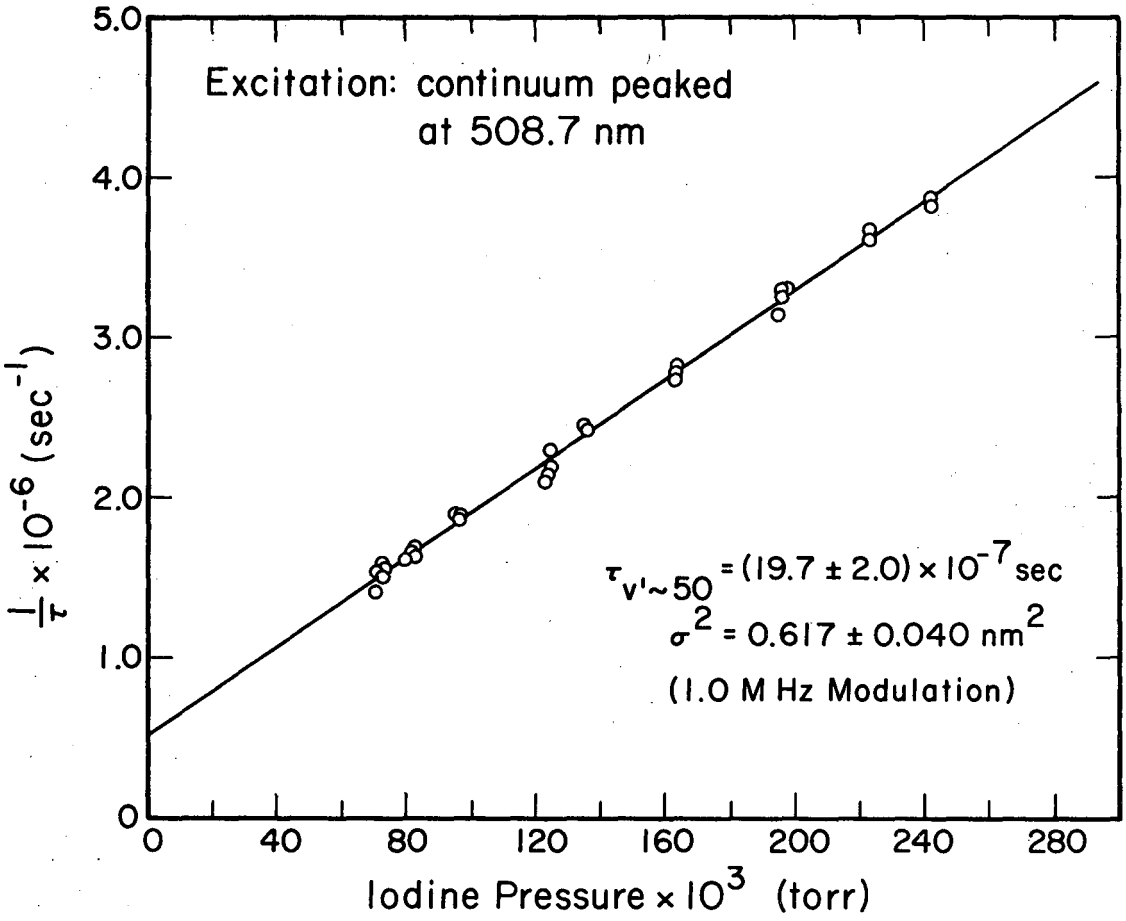

XBL 6810-6019

Fig. II-5

Table II-B. Iodine lifetimes and self-quenching cross-sections

Excitation mode and wavelength (nm)	v'	Lifetimes$\times 10^7$ (sec) [self-quenching cross-sections (nm^2)]			
		This work		Other work	
		1.0 MHz modulation	361 kHz modulation	Chutjian (ref. 6)	Wolff (ref. 8)
589.5 (Na D lines)	15	9.75±0.7 (0.639±0.05)	9.8±0.7 (0.646±0.04)	11.9±0.7 (0.694±0.03)	
589.5 (filtered continuum)	*	9.75±0.7 (0.639±0.05)	9.8±0.7 (0.646±0.04)	11.4±0.6 (0.704±0.04)	8.02±0.55 (0.667±0.03)
546.1 (Hg line)	25	5.75±0.6 (0.617±0.04)	7.4±0.4 (0.668±0.03)	7.13±0.25 (0.630±0.03)	6.28±0.4 (0.729±0.05)
546.1 (filtered continuum)	**	5.66±0.6 (0.601±0.04)	7.4±0.4 (0.668±0.03)	7.69±0.3 (0.674±0.04)	
508.6 (Cd line)	50	15.2±2.0 (0.551±0.04)		53.2^{+8}_{-6} (0.787±0.03)	
508.7 (filtered continuum)	***	19.7±2.0 (0.617±0.04)	20.6±3.0 (0.613±0.04)	42.2^{+7}_{-5} (0.658±0.04)	11.3±0.8 (0.642±0.02)

* v' = 12, 7%; v' = 13, 18%; v' = 14, 17%; v' = 15, 25%; v' = 16, 16%; v' = 17, 8%

** v' = 24, 9%; v' = 25, 26%; v' = 26, 27%; v' = 27, 16%; v' = 28, 10%; v' = 29, 5%

*** Excitation is to a large number of v' levels from 45 to 65 with maximum excitation to v' = 51

$v' \sim 25$ region. These states could either be independent, that is excited separately and decaying with unique but different lifetimes, or cascading may be taking place, in which one state is excited and then decays to other states, with at least two states emitting with wavelengths detectable by the sample photomultiplier. With only two different modulation frequencies it is impossible to sort out even two different lifetimes without knowing the relative signal sizes which radiation from these states would produce in the apparatus. It should be noted that the effect of the possible systematic error in the phase-shifter, which was discussed above, would be to further shorten the lifetime measured at 1.0 MHz by about 3% relative to the lifetime measured at 361 kHz.

Since the review by Chutjian et al.,[101] additional work pertinent to the iodine problem has been reported. The lifetime measurements of Wolff[6] have been mentioned. Ezekiel and Weiss[128] have used the 514.5 nm line from an argon ion laser to excite iodine in a molecular beam to $v' \sim 43$. By pulsing the laser and observing the fluorescence decay they obtain a lifetime of $(30\pm5)\times10^{-7}$ sec. Wassermann et al.[129] have used electron spin resonance to monitor iodine atom concentration in a cell in which iodine molecules are irradiated. They find that iodine atom production is the same for irradiation of the molecules by light of wavelengths longer or shorter than the dissociation limit of the B state, even at low (0.02 Torr) pressures where the degree of collisional predissociation should be small. These results they interpret as evidence for strong spontaneous predissociation.

Chutjian[130] has measured absorption by single rotational lines in 6 bands with $v' = 12, 13, 14, 16, 25$ and 29. Using the measured equivalent width[131] and calculated Frank-Condon factors he has determined the value of

$|R_e|^2$ [see Eq. (II-1)] and the radiative lifetimes for these v'. Finally, preliminary results by Tellinghuisen,[126] who has monitored iodine atom concentration by resonance fluorescence of the 183.0 nm iodine atomic line, indicate that iodine atom production is essentially the same when iodine molecules are irradiated with wavelengths longer or shorter than the dissociation limit of the B state. As with the work of Wassermann et al. mentioned above, this observation persists even at very low iodine pressures where collisional predissociation should be neligible.

The available data on lifetimes and collisional quenching cross sections are collected together in Fig. II-6. Lifetimes based on rotational line absorption measurements by Brown and Klemperer[132] and by Stafford[13] and on broad-band absorption measurements by Stafford[13] were calculated by Chutjian et al.[101] and are included in Fig. II-6.

A few general trends seem to emerge from the data. First, the collisional quenching cross section does not vary widely with changing v'. This indicates that repulsive states crossing the B state do not enhance the probability of collisional predissociation (which is already large) in the region of the crossing. Second, the measured lifetimes are generally shorter than those calculated from absorption data for corresponding v' regions. This indicates that there is another first order process competing with radiative decay. Third, the experiments of Wassermann et al. and Tellinghuisen indicate that the competing process is spontaneous predissociation.

The model which emerges than is one where the B state is embedded in a repulsive state [presumably the $^1\Pi_1+$ state, see ref. (101)] with which there is some slight mixing leading to spontaneous predissociation. Collisions enhance the mixing and give rise to collisional predissociation.

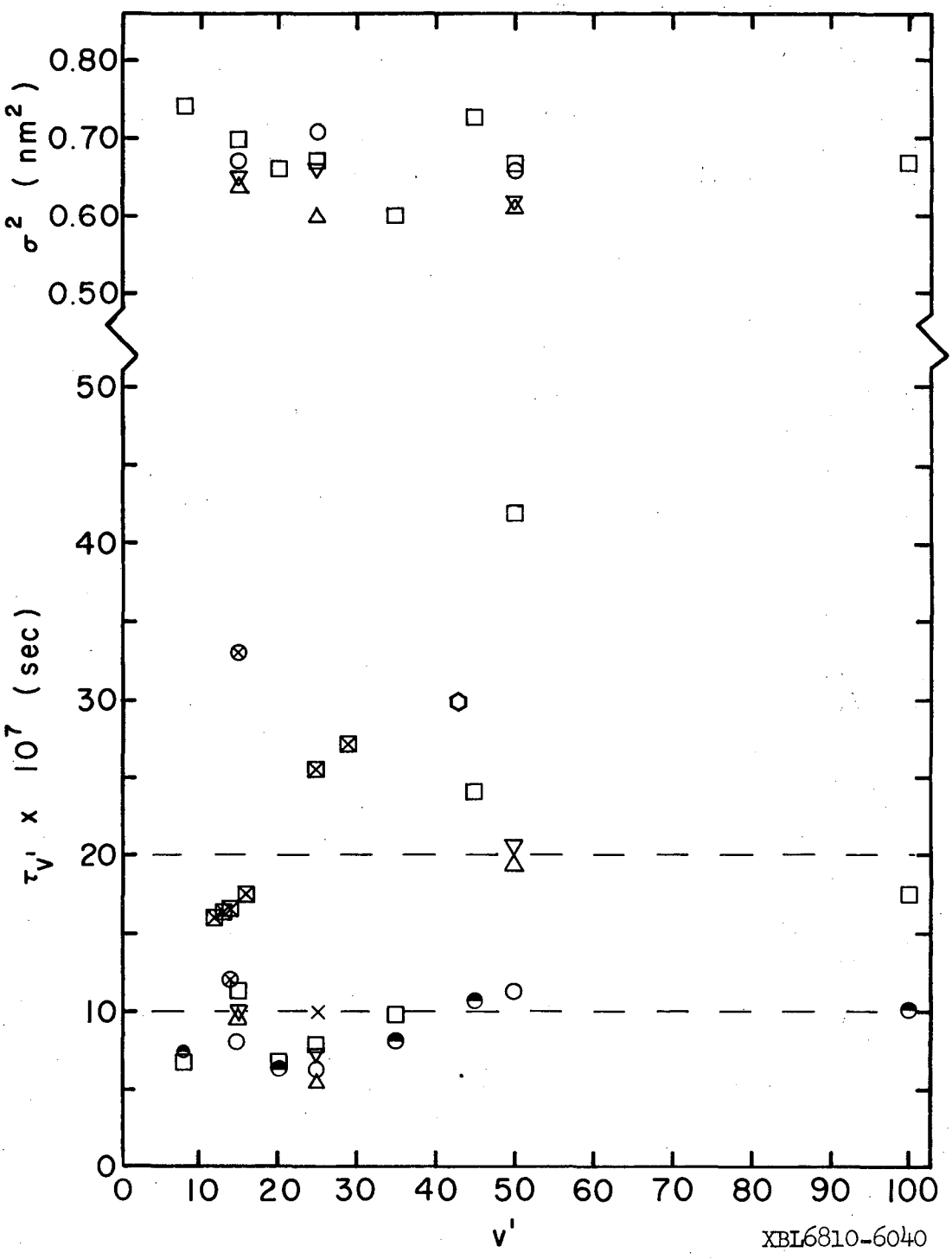
0.80
0.70
0.60
0.50
σ^2 (nm^2)
50
40
30
20
10
0
$\tau_{v'}$ x 10^7 (sec)
0 10 20 30 40 50 60 70 80 90 100
v'
XBL6810-6040

Fig. II-6

Finally, the degree of mixing can vary with the vibration-rotation level of the B state giving rise to quite different lifetimes for nearby levels, thus explaining the variation of measured lifetime with modulation frequency for the $v' \sim 25$ region.

Appendix: Electronic Information

Function	UCRL Drawing No.	Comment
Crystal Exciter	5V1374 and 8S6814A	This RF oscillator-amplifier drives the quartz crystal-transducers in the ultrasonic modulator. Drawing No. 5V1374 is for 5.2 MHz and drawing No. 8S6814A is for 1.0 MHz Operation. Note that the exciter frequency is half the operating frequency.
Photomultiplier Power Supply		One each for reference and sample photomultipliers. Commercial units manufactured by Northeast Scientific Corp. Cambridge, Mass. Model RE3002EW. Insure that the polarity of the high voltage is correct for the particular tube base wiring in use.
Phototube base	8S3493	Use with Amperex 56UVP Photomultiplier tube. Tuned circuit on anode must match operating frequency. When tube is operated with photo-cathode at negative high voltage, the front surface of the tube should be insulated from ground.
Phototube base	8S3483	Use with RCA 7264 and RCA 7265 Photomultiplier tubes. See comments for 8S3493 above.
Reference Channel Chassis (AFC)	8S8603	In 1.0 MHz or 5.2 MHz operation V1 acts as mixer for the reference channel. The tuned circuit on the plate of V6 must match the operating frequency. The tuning fork provides the 1.0 kHz reference signal for the feedback circuit which controls the local oscillator. The local oscillator for 1.0 MHz or 5.6 MHz operation plugs into the top of this chassis. For both ultrasonic and wheel modulation, preamplification of the reference signal is provided
Sample	8S4113	V2 on this chassis is the sample mixer for both 1.0 MHz and 5.2 MHz operation. The tuned circuit on the plate of V1 must match the operating frequency. This chassis also contains the sample amplifier and the sample phase-shifter for all operating frequencies.

Function	UCRL Drawing No.	Comment
Local Oscillator	4V9211 and 8S8611	This chassis plugs into the top of the reference channel chassis and provides the beat signal to reference and sample mixer when using the ultrasonic modulator. Drawing No. 4V9211 is for 5.2 MHz operation and drawing No. 8S8611 is for 1.0 MHz operation.
360 kHz to 1.0 kHz Heterodyne	8S3473	This chassis contains the local oscillator and the reference and sample mixers for 361 kHz wheel operations. R1 and R22 should match input cable impedance. Outputs go to reference and sample channel chassis.
100 KHz to 1.0 kHz Heterodyne	8S3463	This chassis contains the local oscillator and the reference and sample mixers for 99 kHz wheel operation. See comments for 8S3473 above.
Counter		A Hewlett-Packard Model 5245L Counter monitors the 1.0 kHz reference signal to insure frequency stability.
Phase detector	8S4123	This chassis contains final reference signal amplification and the reference channel phase-shifter. It also contains the phase-null detector. Reference signal output is provided to the frequency to voltage convector for wheel operation.
Frequency to Voltage Convector	8S3253A	This unit provides an output to the motor speed control (8S8632). The size of the output signal is controlled by the frequency of the reference channel input from 8S4123. R17 should be adjusted so that ME1 reads about 60-70 volts when the input frequency is 1.0 kHz.
Motor Power Supply	8S8622	This unit provides DC power to the motor for wheel operation. Field voltage connects directly to the motor. A mature voltage goes to the motor speed control (8S8632).
Motor Speed Control	8S8632	This unit regulates the armature voltage from the motor power supply (8S8622) according to the size of the signal from the frequency to voltage converter (8S3253A).

Function	UCRL Drawing No.	Comments
Block diagram for wheel operation	8S8642	This block diagram shows the interconnection of the components when using wheel modulation. A similar diagram for the ultrasonic modulator appears as Fig. I-1 of this thesis.
Spectral Lamp Exciter	8S4092A	This unit provides square wave AC power for the operation of Osram lamps or other spectral lamps which have similar power requirements. The use of square wave AC increases lamp stability and eliminates the 120 cycle ripple produced by line supply.

Acknowledgements

I am grateful to Professor Leo Brewer for his guidance during this work. The opportunity for exposure to his scientific insight and perspective has been exciting and, I hope, not wasted.

My thanks go to all of the members of the research group, particularly to Dr. John Link, and to all of the technicians, machinists, glass blowers, and others who have helped in this work.

I owe very special thanks to my wife, Mary, for her loving confidence and encouragement during this work.

This work was performed under the auspices of the United States Atomic Energy Commission.

REFERENCES

1. A. C. G. Mitchell and M. W. Zemansky, Resonance Radiation and Excited Atoms, (Cambridge University Press, Cambridge, 1961).
2. H. C. Corliss and W. R. Bozmann, Natl. Bur. Std. Monograph 53 (1962).
3. E. W. Foster, Rept. Prog. Phys. 27, 469 (1964).
4. A. Gallagher and A. Lurio, Phys. Rev. 136, A87 (1964).
5. R. G. Bennett, Rev. Sci. Instr. 31, 524 (1963).
6. R. J. Wolff, (Ph.D. Thesis), University of California, Berkeley (1967).
7. E. A. Bailey, Jr. and G. K. Rollefson, J. Chem. Phys. 21, 1315 (1953).
8. A. Chutjian, (Ph.D. Thesis), University of California, Berkeley; UCRL-16441 (January 1966).
9. G. M. Lawrence and B. D. Savage, Phys. Rev. 141, 67 (1966).
10. S. E. Schwartz, (Ph.D. Thesis), University of California, Berkeley; UCRL-18421 (September 1968).
11. A. M. Bronch-Bruevich, Izv. Akad. Nauk S.S.S.R. Ser. Fiz. 20, 591 (1959).
12. R. G. Brewer, (Ph.D. Thesis), University of California, Berkeley; UCRL-8387 (July 1958).
13. F. E. Stafford, (Ph.D. Thesis), University of California, Berkeley; UCRL-8854 (September 1959).
14. R. Berg, (Ph.D. Thesis), University of California, Berkeley; UCRL-9954 (March 1962).
15. L. Brewer, C. G. James, R. G. Brewer, F. E. Stafford, R. A. Berg and G. M. Rosenblatt, Rev. Sci. Instr. 33, 1450 (1962).
16. J. K. Link, J. Opt. Soc. Am. 56, 1195 (1966).
17. P. Debye and F. W. Sears, Proc. Natl. Acad. Sci. U.S. 18, 409 (1932).
18. L. Bergmann, Ultrasonics and Their Scientific and Technical Applications (John Wiley and Sons, Inc., New York, 1938).

97. G. V. Markova and M. P. Chaika, Opt. Spectrosc. 17, 170 (1964).

98. F. Karstensen, Z. Physik 187, 165 (1965).

99. H. Ackermann, Z. Physik 194, 253 (1966).

100. R. J. Wolff and S. P. Davis, J. Opt. Soc. Am. 58, 490 (1968).

101. A. Chutjian, J. Link and L. Brewer, J. Chem. Phys. 46, 2666 (1967).

102. J. K. Link, J. Opt. Soc. Am. 56, 1262 (1966).

103. O. S. Heavens, J. Opt. Soc. Am. 51, 1058 (1961).

104. P. M. Stone, Phys. Rev. 127, 1151 (1962).

105. E. M. Anderson, and V. A. Zilitis, Opt. Spectrosc. 17, 170 (1964).

106. G. S. Kvater and T. G. Meister, Vestnik Leningrad Univ. Ser. Fiz. i Khim. 9, 137 (1952).

107. V. K. Prokof'ev and G. Shtandel, Zh. Eksp. Teor. Fiz. 4, 359 (1934).

108. R. Minkowski and W. Muhlenbruch, Z. Physik 63, 198 (1930).

109. R. W. Schnieder, A. Lurio and W. Happer, Phys. Rev. 173, 76 (1968).

110. G. Stephenson, Proc. Phys. Soc. (London) A64, 458 (1951).

111. H. Bucka, H. Kopfermann and E. W. Otten, Ann. Physik 459, 39 (1959).

112. H. Bucka and G. Oppen, Ann. Physik 465, 119 (1962).

113. J. Cojan and M. Thibeau, Compt. Rend. 249, 1489 (1959).

114. C. J. Schuler, Jr., Quarterly Progress Report Number 74 (Massachusetts Institute of Technology Research Laboratory of Electronics, 1964).

115. A. Lurio, Phys. Rev. 140, 1505A (1965).

116. G. H. Nussbaum and F. M. Pipkin, Phys. Rev. Letters 19, 1089 (1967).

117. H. D. Engler, Z. Physik, 144, 343 (1956).

118. G. D. Bell and R. B. King, Astrophys. J. 133, 718 (1961).

119. M. Z. Khokhlov, Akademii Nauk S.S.S.R. Kryskaia Astrofizicheskaia Observatoriia. Izvestiia 25, 249 (1961).

120. N. P. Penkin and I. Yu. Yu. Slavenas, Opt. Spectrosc. 15, 83 (1963).

121. B. V. Lvov, Opt. Spectrosc. 19, 282 (1965).

122. W. A. Brown, Phys. Fluids 9, 1273 (1966).

123. R. L. de Zafra and A. Marshall, Phys. Rev. 170, 28 (1968).

124. T. M. Helliwell, Astrophys. J. 133, 566 (1961).

125. P. A. Rice and C. V. Ragone, J. Chem. Phys. 42, 701 (1965).

126. J. B. Tellinghuisen, Private Communication.

127. D. A. Shirley and W. F. Giauque, J. Am. Chem. Soc. 81, 4778 (1959).

128. S. Ezekiel and R. Weiss, Phys. Rev. Letters 20, 91 (1968).

129. W. Wassermann, W. E. Falconer and W. A. Yager, Berichet der Bunsengesellschaft 72, 248 (1968); J. Chem. Phys. 49, 1971 (1968).

130. A. Chutjian, Private Communication.

131. J. B. Tatum, Astrophys. J. Suppl. Ser. 14, 21 (1967).

132. R. L. Brown and W. Klemperer, J. Chem. Phys. 41, 3072 (1964).

FIGURE CAPTIONS

Fig. I-1 Block diagram of 5.2 MHz (or 1.0 MHz) apparatus. Components in the optical path are: R, source of exciting radiation; L_1, L_2, L_3 and L_4, lenses; F_1 and F_2, filters for wavelength isolation; UT, ultrasonic grating (tank); A, aperture stop; G_1 and G_2, multiple slits; GP, glass plate; S, sample. The electronic components are described in the appendix.

Fig. I-2 Diagram of the ultrasonic grating (tank). A, body of the tank; B, copper reflecting plate; C, threaded cap to hold windows (L_2 and L_3 in Fig. I-1) on tank; D, quartz crystal-transducer; E, Lucite disk; F, threaded ring to press Lucite disk in place.

Fig. I-3 Equivalent circuit for calibrated phase shifter. e_s and e_o, input and output signals respectively; R_s, source impedance of cathode follower; R, variable resistance; C, fixed capacitance.

Fig. I-4 Error in $\Delta\phi$ introduced by neglect of cathode follower source impedance versus value of R (see Fig. I-3) in calibrated phase shifter. $\Delta\phi$ for $R_s = 0$ is given on upper abscissa.

Fig. I-5 Atomic beam assembly. A, beam chamber; B, cooling water jacket; C, side arms for entrance and exit windows; D, liquid nitrogen trap; E, beam shutter; F, frosted glass plate; G, position of fluorescence viewing window in front and outlet to diffusion pump in back; H, water

cooled electrodes; I, tantalum resistance heater; J, sample crucible; K, radiation shield; L, roughing pump outlet.

Fig. I-6 Diagram of the aluminum flow lamp drawn approximately to scale. A, Pyrex body of the lamp; B, necked down region of the lamp enclosed by microwave cavity; C, helium inlets; D, adjustable support for heating element and crucible; E, outlet to pump; F, quartz window.

Fig. I-7 Experimental τ_k values for the 7s $^2S_{1/2}$ state of Tl. The solid curve is calculated using Eq. (I-6) and a true lifetime, τ_k°, of 7.65 nsec. Entrapment starts where $(1 + L_f/L_n) \simeq 500$.

Fig. I-8 Experimental τ_k values for the Ag ($0.9\ \tau\ ^2P_{1/2} + 0.1\ \tau\ ^2P_{3/2}$) measurement (see text). The solid curve is calculated using Eq. (I-6) and a true lifetime, τ_k°, of 7.4 nsec. Entrapment starts where $(1 + L_f/L_n) \simeq 80$.

Fig. I-9 Atomic energy levels and transition wavelengths, given in nm, for all states studied. The energy level spacings are drawn to scale. The $^2P_{1/2}$ to $^2P_{3/2}$ level spacing is given in electron volts for Al, Ga, In, and Tl.

Fig. II-1 Plot of the difference between the calculated and measured phase-shift for delay lines versus the calculated shift. The reason for the difference is not known but may represent systematic error in the calibrated phase-shifter.

Fig. II-2 Plot of $1/\tau$ versus iodine pressure for filtered continuum excitation peaked at 589.5 nm and for 1.0 MHz modulation.

Fig. II-3 Plot of $1/\tau$ versus iodine pressure for 546.1 nm Hg line excitation and 1.0 MHz modulation.

Fig. II-4 Plot of $1/\tau$ versus iodine pressure for combined filtered continuum and Hg line excitation at 546.1 nm and 361 kHz modulation.

Fig. II-5 Plot of $1/\tau$ versus iodine pressure for filtered continuum excitation peaked at 508.7 nm and 1.0 MHz modulation.

Fig. II-6 Plot of available iodine lifetimes and collisional quenching cross sections for various v' regions.

- Δ phase-shift lifetime 1.0 MHz modulation (this work);
- ∇ phase-shift lifetime 361 kHz modulation (this work);
- $\square$ phase-shift lifetime 359 kHz modulation (ref. 8);
- O direct decay lifetime (ref. 6);
- ● direct decay lifetime (preliminary data ref. 6);
- ⬡ direct decay lifetime (ref. 127);
- ⊠ rotational line absorption (ref. 129);
- O rotational line absorption (ref. 132, see text);
- X rotational line absorption (ref. 13, see text);
- ⁚⁚⁚ limits of band absorption (ref. 13, see text).

TECHNICAL INFORMATION DIVISION
LAWRENCE RADIATION LABORATORY
UNIVERSITY OF CALIFORNIA
BERKELEY, CALIFORNIA 94720